# Electronics for High Energy Particle Detection

*Erik Margan*
R&D Eng., Experimental Particle Physics Department, Jožef Stefan Institute, Ljubljana, Slovenia

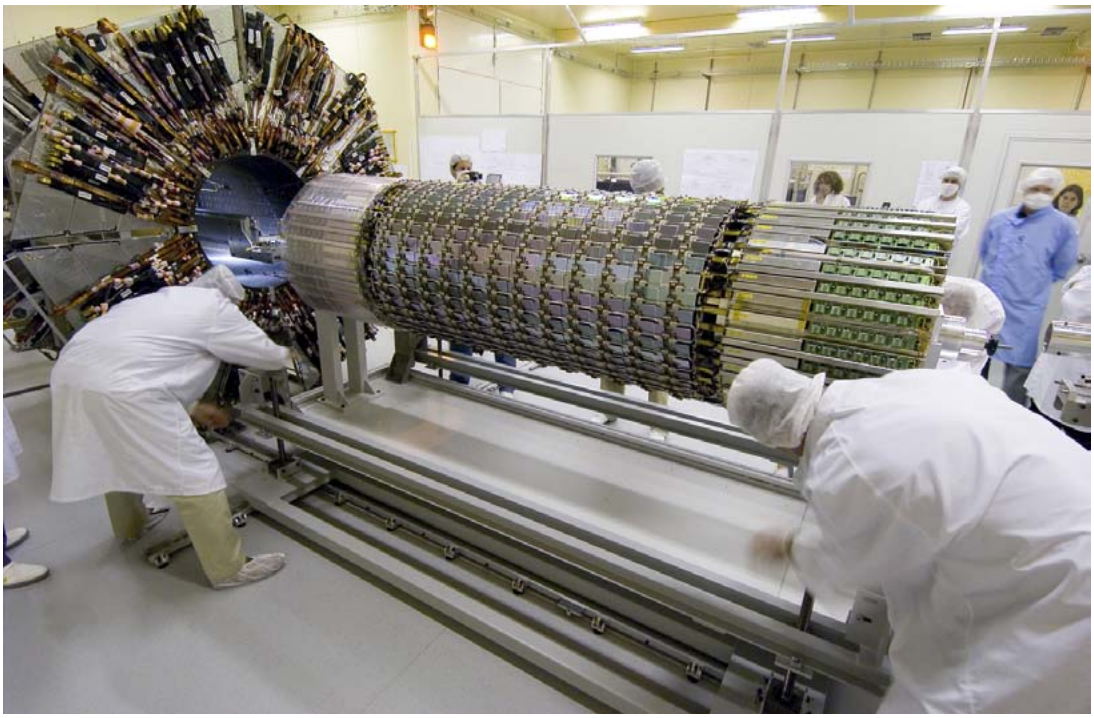

**Fig.1:** Clean room last checking of the Silicon Tracker (SCT) before its installation into the inner detector of ATLAS, one of the four major experiments of the Large Hadron Collider (LHC) at CERN.

**Abstract:** In the past 30 years we have seen a revolution in front-end electronics for large scale detector systems applied in high energy particle detection. Custom integrated circuits, specifically tailored to large detector system requirements, have provided unprecedented performance and enabled the construction of systems that were once deemed impossible. The evolution of integrated circuits in strip and pixel detector readout is reviewed, some present applications in the Large Hadron Collider (LHC) described, and the challenges posed by the future Super-LHC and the International Linear Collider (ILC) are indicated. Performance requirements are constantly increasing, but key considerations remain more or less unchanged: signal to noise ratio, power dissipation, signal acquisition, and data processing.

**Introduction**

Let me be allowed to skip the usual introductory poetry on how magnificent is the view of the clear night sky full of stars, and how equally amazing is the mere fact that we ourselves are but the stardust, and how remarkable is our insight that it is possible to learn how this incredibly vast Universe came to be by probing the atomic and subatomic levels of existence.

Let me also be allowed to skip the usual quoting of old Greek philosophers, as well as the usual historical stream of important scientific discoveries.

The deepest secrets of Nature are mysterious when we do not know them, but we find them almost trivially simple once we discover their inner working. In contrast, much more interesting and fun is the way and the means by which we have sometimes ingeniously managed to convince Nature to reveal one or two of Her hidden bits.

Recently the startup of the CERN's [1] Large Hadron Collider (LHC) [2] has caught the public attention, not just because it represents a new landmark in particle physics, as well as science and engineering in general, but more for a doomsday scenario, advertised by some either ill-informed, or worse still, panic spreading freaks, that the colliding particles would create a micro black hole [3], which would quickly grow and ultimately swallow the Earth. It is probably not worth trying to reassure people that the Earth's upper atmosphere is being bombarded constantly, day and night, by cosmic particles with energies around $10^{18}$ eV, occasionally even $10^{21}$ eV [4] (that is 8 orders of magnitude greater than the humble $1.4{\times}10^{13}$ eV of the LHC at full power), and we are still here! OK, some theories do predict the formation of micro black holes well within the energy range of the LHC, but according to those same theories, small black holes 'evaporate' more quickly the smaller they are (owed to the *Hawking–Beckenstein* radiation [5]). Those formed by the LHC will therefore disintegrate into a shower of particles almost in the instant of creation, within a time interval between $10^{-35}$ s and $10^{-43}$ s (Planck's minimum quantum action time [6]).

Such alarms would have been quite funny if they were not a clear warning of the sad state of scientific knowledge among the general public, as well as of the distrustful image of scientists and engineers in general, who are often pictured as childish, slightly 'nuts', socially irresponsible, or even openly mad and malevolent individuals, ready to do anything in order to realize their own selfish goals.

To be honest, one has to be more than just slightly nuts to work 16 hours a day for the miserable wages the government agencies and institutes worldwide are paying for scientific work. And anyway, I myself would be horrified if people around me would see me as 'serious' or 'rational'. As *Douglas Adams* has put it wisely in his *Hitchhiker*'s *Guide to the Galaxy* : *"I'm a scientist and I know what constitutes proof; but the reason I call myself by my childhood name is to remind myself that a scientist must also be absolutely like a child. If he sees a thing, he must say that he sees it, whether it was what he thought he was going to see or not. See first, think later, then test. But always see first. Otherwise you will only see what you were expecting. Most scientists forget that. [...] So the other reason I call myself Wonko the Sane is so that people will think I am a fool. That allows me to say what I see when I see it. You can't possibly be a scientist if you mind people thinking you're a fool."*

[1] D. Adams: The Ultimate Hitchhiker's Guide, Part 4: So long, and Thanks for All the Fish, Chapter 31

Anyway, I think that more knowledge (not necessarily the mathematical type!) won't do people any harm, and might also alleviate those crude stereotypes about scientists and engineers, if ever so slightly.

So let me be allowed a quickly flyby over some basic physics, the properties and configuration of silicon detectors, and finally showing you some relatively simple circuit diagrams. If you are still with me, then you probably are an electronics enthusiast, perhaps even a passionate circuit designer, like I am. Therefore please be warmly and friendly welcome to the fascinating field of detector electronics!

**Basic Physics**

Detecting subatomic particles is a demanding task. In order to be able to identify exactly what is going on in a particular physical event on a quantum scale, you must first know your colliding input quantities. Then you must be able to collect all the resulting debris, measure all the masses ('rest' internal energies), the kinetic energies, the electric charge or the lack of it, trace all the trajectories, and find out whether and which ones of those particles originate from the primary event or one of several secondary decay showers. Finally, you have to account for known quantum processes, examine the energy balance in detail, and check if all adds up or if something is curiously missing.

Then you need to record a large number of similar events to improve the statistics and reduce any background noise, extrapolating for the missing parts. Only then can you actually start your analysis, trying to match the theory to the experimental data. If you are lucky, then probably Nature has been looking kindly to your efforts, allowing you to peer through a keyhole and see Her shadow while She was changing clothes. If you are not lucky, you have been following some already known or unimportant trivia, and you have spent an awful lot of time in vain.

The four known natural forces form the ratio $1 : 10^{-2} : 10^{-12} : 10^{-40}$, with the strong nuclear force as the reference, the electromagnetic force, the weak nuclear force and the gravitation force, respectively. However, both nuclear forces are evident only at a very short range, comparable to a size of a nucleus, because they fall off with distance more quickly then electromagnetic and gravitation forces (which, as is well known, exhibit a $1/r^2$ law).

Thus the dominant electromagnetic phenomena govern many aspects of particle behavior after the collision. For example, in a homogeneous magnetic field, the electrically charged particles follow curved paths, the curving direction being dependent on the polarity of their charge, whilst the curvature radius is proportional to the particle mass and kinetic energy, and inversely proportional to the magnetic field strength. In contrast, neutral particles travel in a straight line.

The outreach of a particle is proportional to its mass and kinetic energy, and is inversely proportional to the specific absorption characteristics of the material they go through. The outreach is also inversely proportional to particle lifetime (in case of metastable particles, which usually decay into more stable ones). All this helps us to identify the most common particles (photons, electrons, protons neutrons and some mesons) and allows us to discriminate between them. For other particles many more complex identification tests must be performed [7].

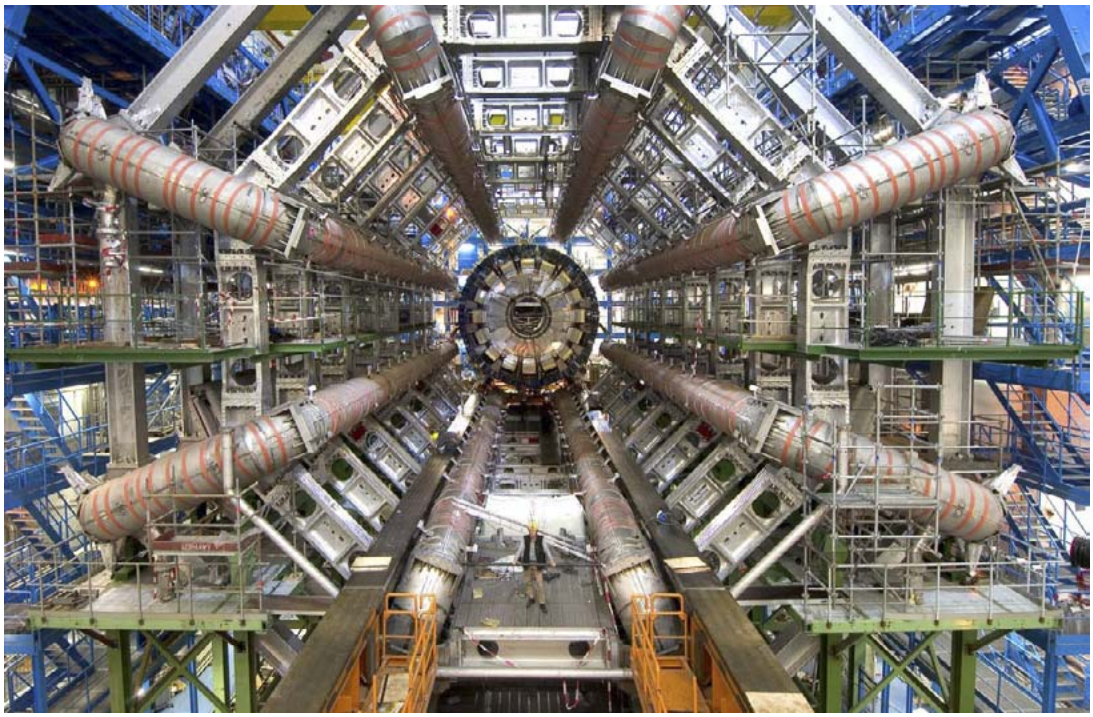

**Fig.2:** Probably the most popular photograph (August, 2006) of a particle physics facility ever made. The inner detector is sliding into its place between the eight superconducting coils which will sustain the toroidal magnetic field for the ATLAS experiment. ATLAS is one of the four main experiments within the LHC (the other three are CMS, ALICE, and LHCb).

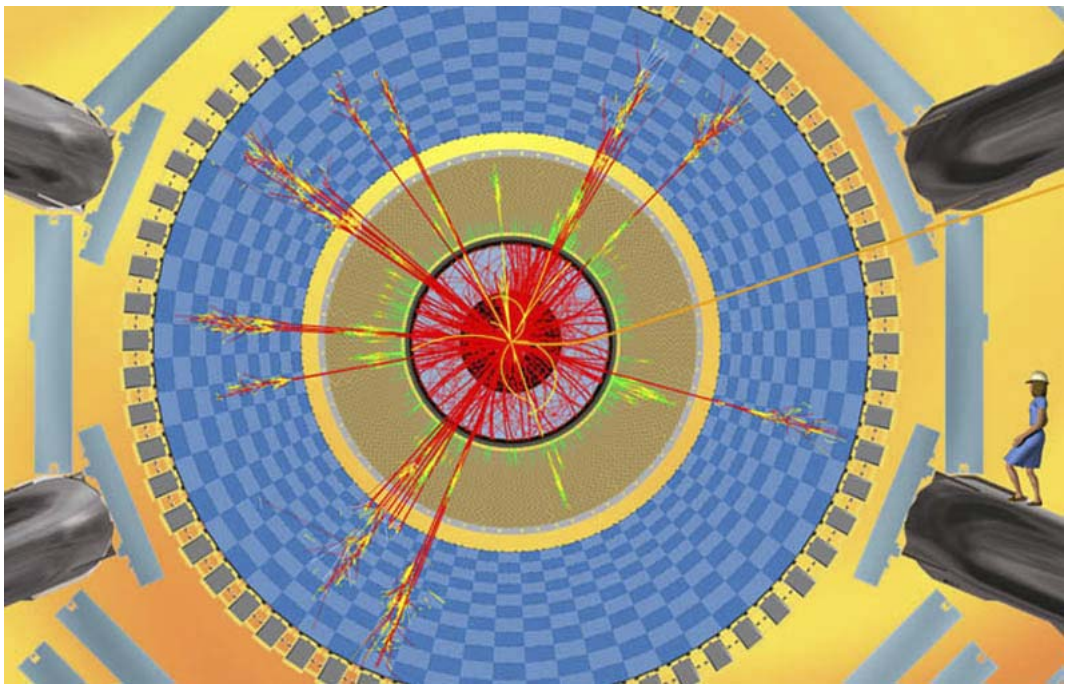

**Fig.3:** Computer simulation of one of the many possible ways a micro black hole, created in a collision, would decay into a shower of particles, as might be detected by ATLAS. At each interaction with the detectors the particles will lose some energy and decay into secondary showers, until finally being absorbed in the calorimeters.

In order to understand the basics of particle physics research we need to bear in mind only two simple mathematical relations and two simple physical processes. The actual physics behind them is relatively complicated, and to our fathers it must have been incomprehensible, but today those relations and processes are part of the general culture and we accept them almost without thinking. So I'm sure that this and the following page will be easy to understand by everyone. If, nevertheless, you fail to understand them, it will probably be because I was oversimplifying things; in this case please see the relevant references.

What is the point of smashing particles at high speed, anyway? Does it mean that the resulting debris were actually hidden inside the colliding particles, and that the collision broke the envelope, releasing the content out?

No!

By accelerating a particle to a very high speed, close to the speed of light, the particle gains a kinetic energy, which is added to its own internal ('intrinsic', 'rest') energy. The most popular physics equation of all times, usually attributed to *Albert Einstein*, but actually known already to *Jules Henri Poincaré*, relates closely energy and mass via a simple proportionality constant [8]:

$$E = mc^2 \tag{1}$$

This relation tells us that a particle at rest (relative to our laboratory) will exhibit a property called mass, with a value equivalent to its internal energy content divided by the speed of light squared. It also means that any kinetic energy administered to that same particle will increase its total energy, which can be interpreted as an effective increase of its mass. Finally, the most profound meaning of this equation is that energy to mass conversion (and back!) is a basic natural process.

Two well known effects can nicely illustrate this last point. One is the production of pairs of complementary charged particles [9]. For example, if a high energy ( $> 1.022\,\mathrm{MeV}$) photon $\gamma$ passes close to a proton p (within its strong magnetic field), the electromagnetic energy of the photon is converted to an electron–positron pair ($e^-$, $e^+$), each of them taking half of that energy ($511\,\mathrm{keV}$), whilst any excess energy is converted to their acceleration, taking them away from each other. In this reaction the proton remains unchanged, it acts almost as some kind of a 'catalyst', providing only the suitable 'environment' in which the reaction takes place:

$$\gamma + \mathrm{p} \rightarrow \mathrm{e}^+ + \mathrm{e}^- + \mathrm{p} \tag{2}$$

The other well known effect is the reverse of this same process, that is the electron–positron annihilation [10] into a pair of photons:

$$\mathrm{e}^+ + \mathrm{e}^- \rightarrow \gamma + \gamma \tag{3}$$

This process we exploit in medical imaging (positron-emission tomography, PET [11]). But these are only two examples, others include various types of nuclear synthesis (in stars) or decay, the nuclear bomb being probably the most dramatic.

Back to accelerated particles, we ask ourselves how much energy can be gained by speeding up a particle. This is governed by another well known relation, the *Lorentz–FitzGerald* transform for the effective (relativistic) particle mass [12]:

$$m_r = m_0 \frac{1}{\sqrt{1 - \frac{v^2}{c^2}}} \tag{4}$$

Here $m_r$ is the effective relativistic mass of a particle with a rest mass $m_0$ when it is moving at a speed $v$, compared to the speed of light $c$. As an example, if we accelerate a particle to 99% of the speed of light, $v/c = 0.99$, the mass effectively increases by a factor $m_r/m_0 \approx 7$; if, however we accelerate a particle to within 1 ppm of $c$, 99.9999%, the mass increases by a factor $m_r/m_0 \approx 707$. Theoretically, any particle moving at exactly the speed of light would have an infinite effective mass (thus infinite kinetic energy), which would require infinite acceleration energy, which in turn has led Einstein to conclude that the speed of light is the absolute upper speed limit in nature (yes, there are some absolutes even in the Theory of Relativity!).

So by colliding high energy particles, in accordance with equation (1), we achieve a huge spatial concentration of energy, which then becomes available for the **creation** of anything that exhibits a certain amount of stability (within the available energy), even if for a femtosecond only. The higher the collision energy, the closer we get to the 'Big Bang'. The laws of thermodynamics and many astronomical measurements (most importantly the cosmic microwave background, discovered by *Penzias* and *Willson* in 1965 [13]) suggest that the Universe upon creation was expanding and cooling down through a series of balanced states [14] with energy converting to matter and back, until finally the available average photon energy became lower than that required for the $e^+$, $e^-$ pair creation, so stable atoms were able to form, the light decoupled from matter, and the Universe became transparent for electromagnetic radiation. One of the best texts ever written on this subject is *The First Three Minutes* [15] by the Nobel laureate *Steven Weinberg*, and I warmly recommend it to readers not familiar with these ideas.

The study of high energy collisions allows us to probe the eventual existence of particles which were dominant at that particular epoch in the history of the Universe, related to that particular energy range. When such 'islands of stability' are discovered, we study the behavior of those particles, seeking for the underlying laws of physics common to all known ranges of particles and energies. The ultimate aim is to discover those universal laws governing and leading to this exact outcome of that spectacular event at the beginning of time.

Now, what is it all good for? What's in it for you and me? At this point it might be important to stress that, beyond the pure knowledge, fundamental research has always been extremely fruitful in applications, too, although mostly in the long run. But any research project also poses many immediate technical and technological requirements, which need to be solved in the first place to build the necessary research tools, leading in turn to many immediately usable products or technological processes. Finally, basic research occasionally produces completely unexpected findings as a side result, which often open whole new areas for both new research and new applications (in CERN they like to point out that the World Wide Web was invented there).

Some people might argue: "Still, in early 1990s the American Congress canceled their Superconducting Super-Collider (SSC), because the project was too expensive! How much did the LHC cost to build, and how did the member states of CERN manage to handle the expenses?"

First, the LHC is truly a global project, whilst the SSC was a single nation project (although USA would have certainly been capable of covering the final cost even if it doubled, it is a question whether there would have still been possible to achieve a general political consensus at a later date). Next, the SSC was canceled partly because the LHC was already going strong, even if the Large Electron–Positron collider (LEP) was still running at that time (until November 2000). Although only slightly smaller than the SSC, the LHC was much cheaper because it was going to use the existing LEP tunnel, and only the caverns harboring the new experiments had to be constructed. Next, more than half of the cost of the LHC has been returned to the member states in form of orders for their own industries to supply the required hardware and instrumentation. Then, the required scientific work force employed was on the pay list anyway, and CERN with all its activities was the perfect environment for many graduate, post-graduate and post-doc students, who took their own part in preparing everything from documentation to instrumentation. Although the initial cost of the LHC has also substantially increased over the years, amounting to the final $\sim 6\,000\,000\,000$ €, the specific cost was not very high: divided by the population of the participating states, it amounted to roughly a single cup of coffee per person per year for the last 14 years! At the same time, the high-tech industries of many countries got jobs, developing technologies, which will form the base of many future products [16]. And we will soon get the computing GRID [17]. And as a bonus we will learn what exactly has been going on immediately after the birth of the Universe [18].

Not bad for 14 cups of coffee, eh?

### Silicon Detectors

Today the most precise measurements of particle energy, as well as the most precise reconstruction of their path, is done with silicon-based detectors. Silicon detectors are relatively large wafers on which an array of diode-like structure is formed. According to the form of those arrays, there are two basic detector types: the pixel type and the strip type, each with its own advantages and disadvantages.

Fig.4 shows a schematic cross-section of a typical silicon strip detector.

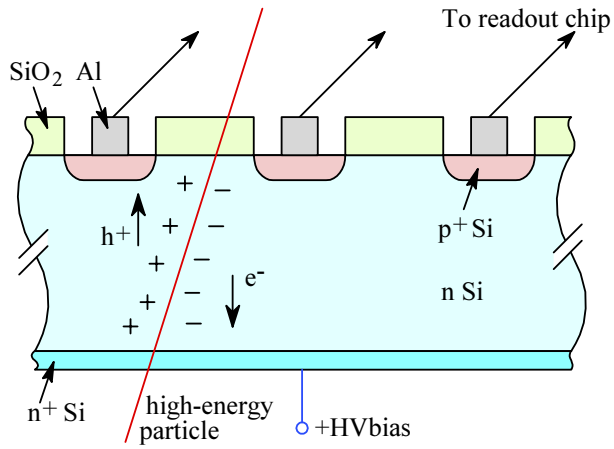


**Fig.4:** Schematic cross-section of a typical silicon strip detector.

Electronics engineers may find a great similarity between such a detector and a more familiar photo-diode; in fact, these detectors are also sensitive to photons. The reverse bias voltage completely depletes the bulk material of charge carriers by a high gradient field. Within this field, the charge, created by ionization after the transition of a high energy particle, will quickly drift towards the appropriate electrodes, where it is collected to produce a fast but weak electric signal. This signal, a current pulse, is then amplified and processed by the readout chip.

Initially, when introduced in 1951 [19], silicon detectors were used primarily to measure the energy of particles from a nuclear decay, and only later, in early 1970s, arrays of such simple detectors were used to also read the position and volumetric distribution of particle showers [20]. The introduction of planar processing technology allowed large wafers to be appropriately segmented and produced cheaply on a large scale [21], [22]. This enabled the production of large area, high resolution detectors for accurate position definition. Multiple layers of such detectors were in turn used to reconstruct the particle trajectories, as well [23].

Silicon detectors are an attractive choice in particle physics because of their excellent intrinsic energy resolution: one electron–hole pair is produced by every 3.6 eV released by a particle crossing the medium. This is a very low value, compared to the 30 eV required to ionize a gas molecule in a gaseous detector, or ~300 eV to extract an electron from a photocathode coupled to a plastic scintillator. Also, the high density of the silicon medium reduces the range of excited secondary electrons, allowing good spatial resolution. Another desirable property of the high density of silicon is its high energy loss, about 390 eV/μm, giving about 108 (e–h)/μm.

However, unlike in other detectors, silicon does not exhibit multiplication of primary charge; the collected charge is a function of detector thickness only. Silicon detectors are installed close to the interaction point, where a thick material can spoil the impact parameter measurement. To minimize multiple *Coulomb* scattering, the material thickness should be as low as possible. A practical limit is set by the signal to noise ratio. Typically, a thickness of 300 μm gives an average of $3.2\times10^4$ e–h pairs.

Such a signal is easily detectable by ordinary low noise electronics. But most of the background noise comes from the intrinsic carrier density in silicon, about $1.45\times10^{10}$ per $cm^3$ at room temperature. In a volume of silicon with an area of 1 $cm^2$ and 300 μm thickness there are some $4.5\times10^8$ thermally excited free charge carriers, which is ~$10^4\times$ larger than the expected signal. In doped silicon, with more free carriers, the signal to noise ratio is even worse.

The signal to noise ratio can be improved by cooling the detector, but this is not always practical. Fortunately, it is easy to reduce the number of free carriers by applying a reverse bias to the PN junction, with a voltage high enough to fully deplete the detector. A depleted detector behaves like a very high resistance, conducting little leakage current (ideally none), but once a particle ionizes the crystal, the induced carriers drift in this high electric field towards the junction where they are collected.

Pixel detectors, as the name suggests, are 2D arrays of small active areas, and, being small, they are ideal as detectors, mainly because of their low capacitance, and consequently low noise. But they require a huge amount of processing electronics. For example, an area of, say, 50×50 $mm^2$, covered by 100×100 $\mu m^2$ pixels, amplified individually, would require 500×500 = 250 000 amplifiers! Serial readout, similar to

that in CCD image cameras, reduces this number substantially. In contrast, a strip detector of roughly the same dimensions and with a strip pitch of 100 µm would require only ~500 amplifiers for direct readout. To obtain a 2D coordinate position of the particle, two such structures must be mounted in a back-to-back 'sandwich' with perpendicular orientation of strips to form a matrix. This doubles the amplifiers to ~1000, though still less than required by a pixel detector.

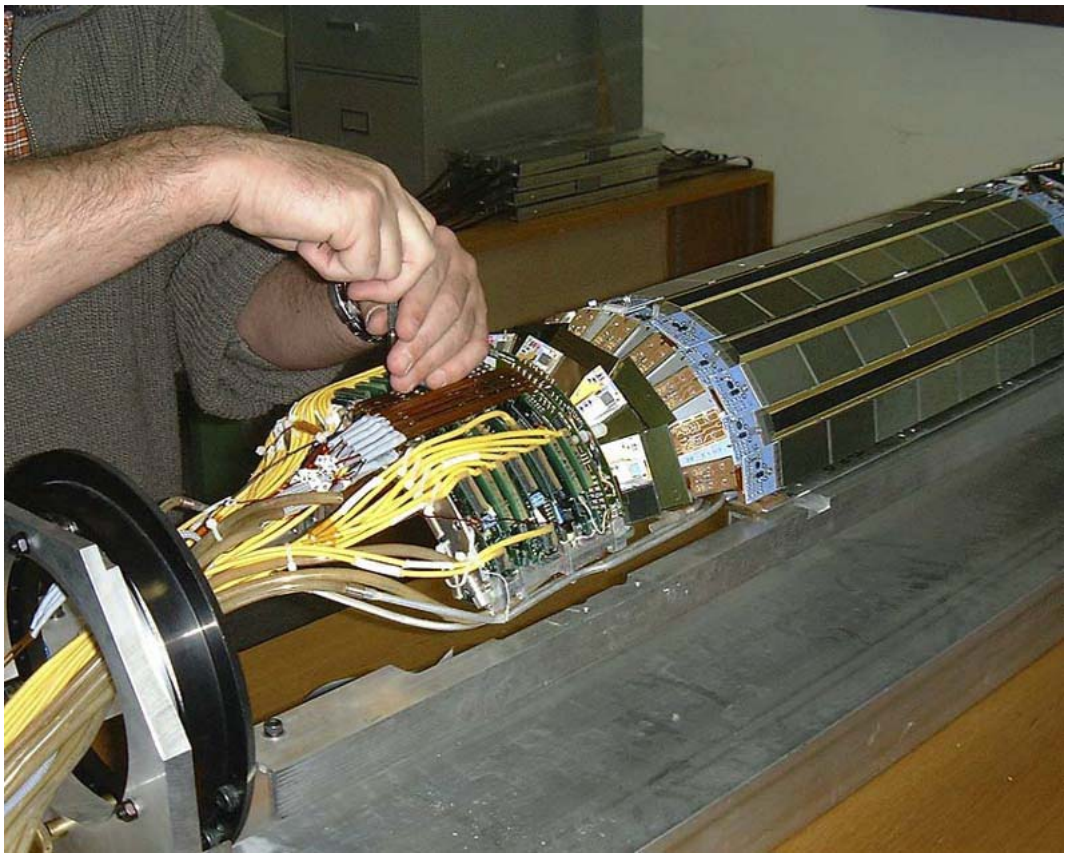

**Fig.5:** One half of the Silicon Vertex Detector [24] of the LEP DELPHI experiment [25-29], after the dismantling in December 2000 [30]. Pixel detectors form the middle 'barrel'. The angled sections (two on each side) form the Very Forward Tracker [26], consisting of pixel detectors (inner layers) and strip detectors (outer layers).

The number of amplifiers is important, since those amplifiers must process short pulses, consequently their power consumption tends to be high. Although the power is optimized by a trade off between bandwidth and noise, the sheer number of amplifiers results in chips running hot. Also, because we want to cover the whole area of interest with at least three layers of detectors (to be able to reconstruct the particle track's curvature), the system power dissipation is an important factor. Tight packing of components creates cooling problems, so the whole geometry must be optimized.

In practice, the number of amplifiers required by the strip detector can be halved or the spatial resolution improved by laying out 'interpolation' strips between the readout strips, and use a suitable reconstruction algorithm for the analysis of the charge distribution in adjacent strips near the hit. I.e., by using a 200 µm readout pitch, the presence of interpolation strips between the readout strips allows a spatial resolution improvement from about 90 to only 26 µm. On the other hand, the increase in noise because of increased stray capacitance reduces it to about 35 µm.

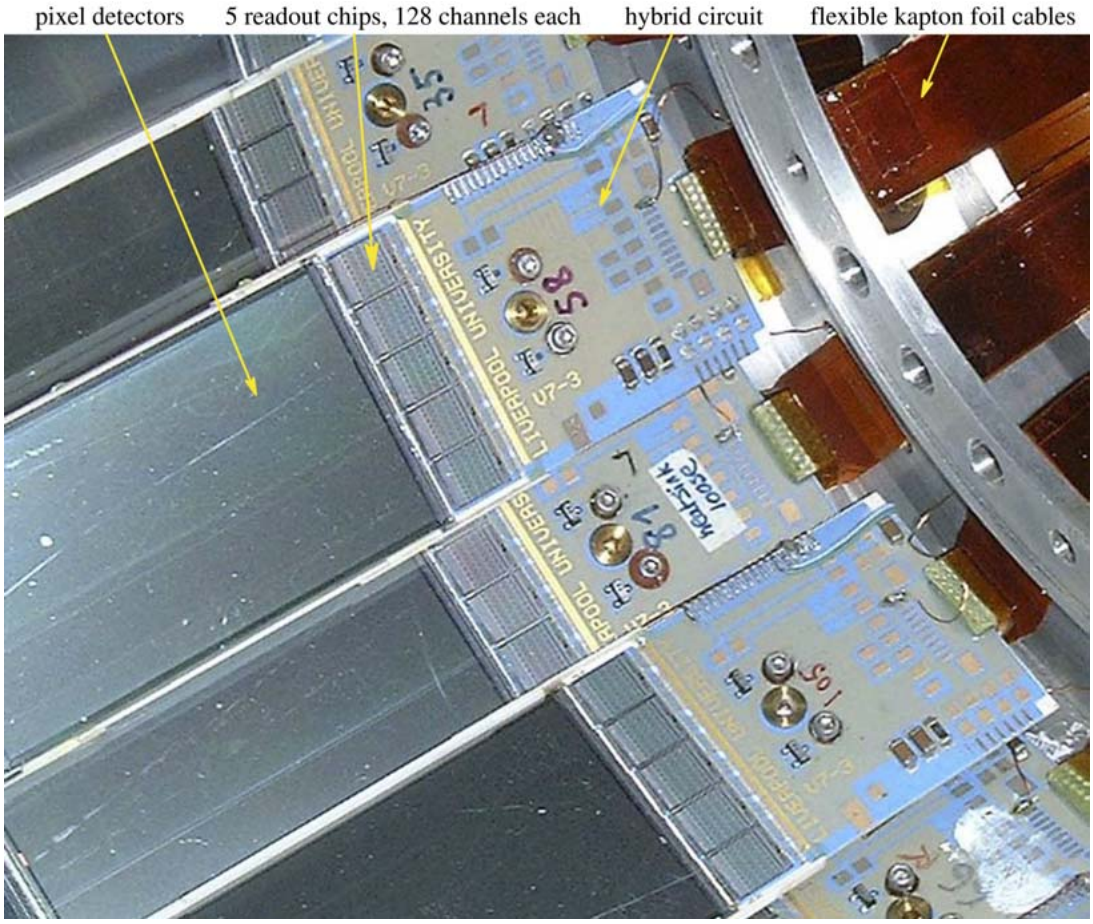


**Fig.6:** LEP DELPHI Vertex pixel detector modules (inner view). Each detector is read by 5 chips, each chip has 128 charge sensitive amplifiers and a cascadeable serial readout.

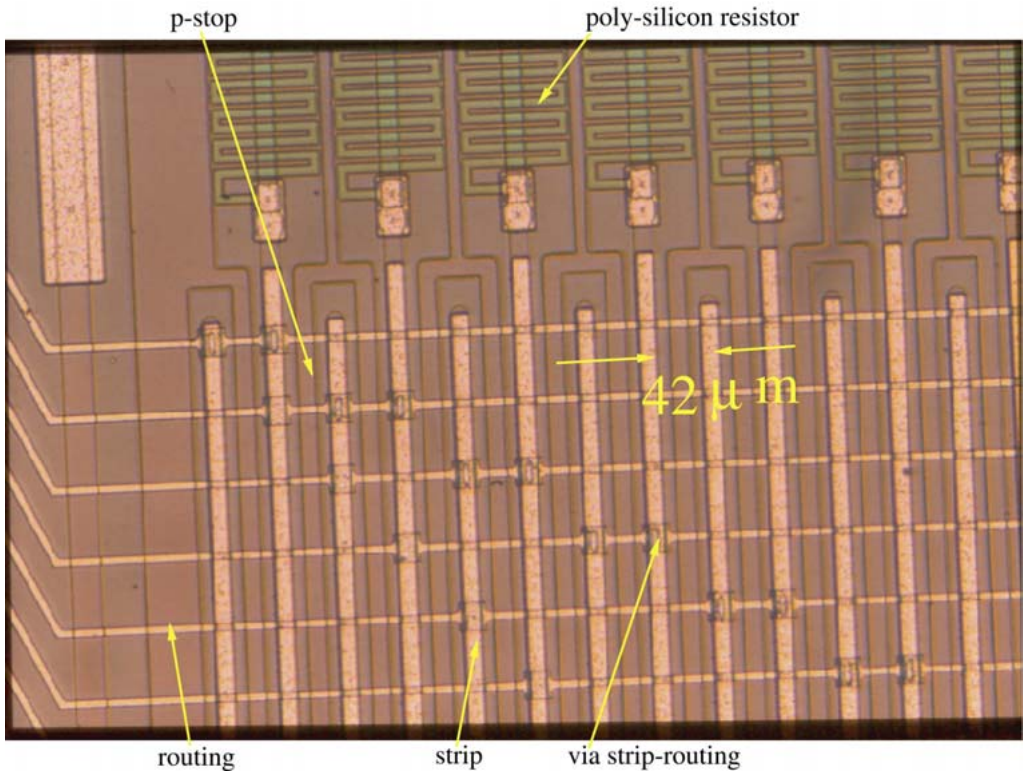


**Fig.7:** Microscopic view of one of the DELPHI Vertex pixel detectors, produced by Hamamatsu

The charge collected by the interpolation strip is capacitively coupled to the readout strips, improving position accuracy. But this charge is taken away from the readout strips, reducing the signal amplitude and lowering the signal to noise ratio. Charge collection can be increased by increasing the strip width, but then the capacitance loading the amplifier input also increases, lowering again the signal to noise ratio. Thus the actual configuration used is always a choice of judicious compromise. Fig.8 shows a cut of a typical strip detector.

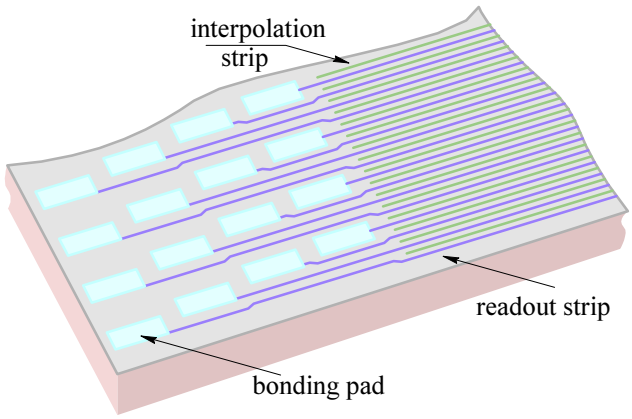


**Fig.8:** A cut corner detail of a typical strip detector die. The pitch of the readout strips can vary from 25 µm without interpolation strips to 200 µm with one or two interpolation strips between each readout strip pair. The strip width is usually 30% of the spacing, their length can be 50 mm or more. The detector thickness is 300 µm.

Strip detectors, similar to that shown in Fig.8, were mounted in the Very Forward Tracker (VFT) [26], Fig.10, as part of the upgrade of the DELPHI [25-30] experiment of the old Large Electron–Positron (LEP) collider [26].

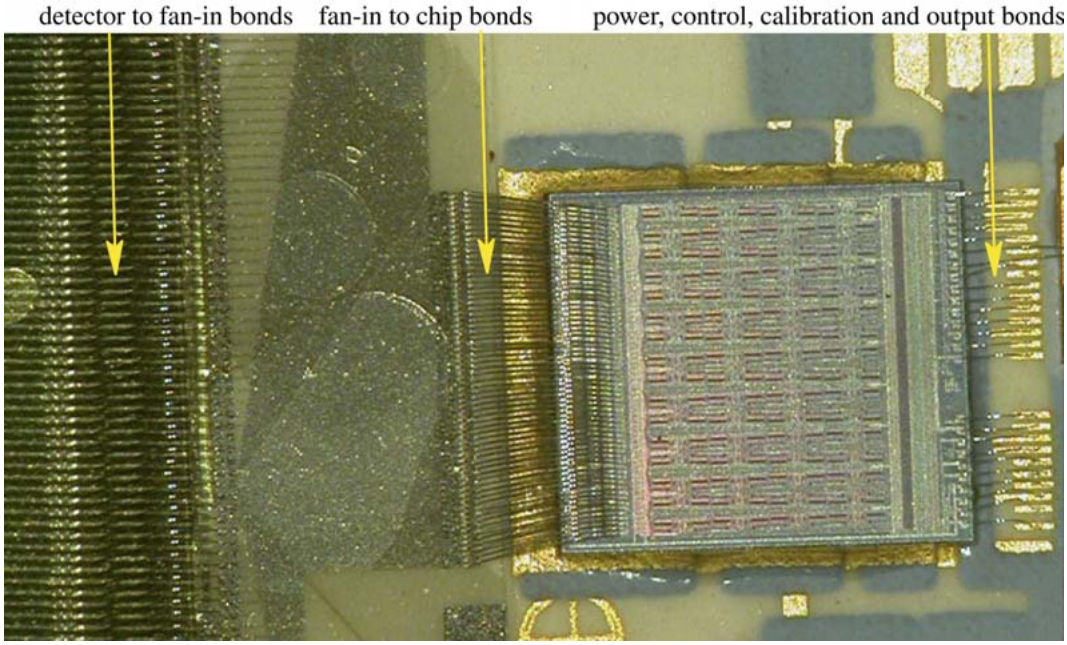


**Fig.9:** The bonding of the MX6 readout chip, used in the VFT of the LEP DEPLHI experiment.

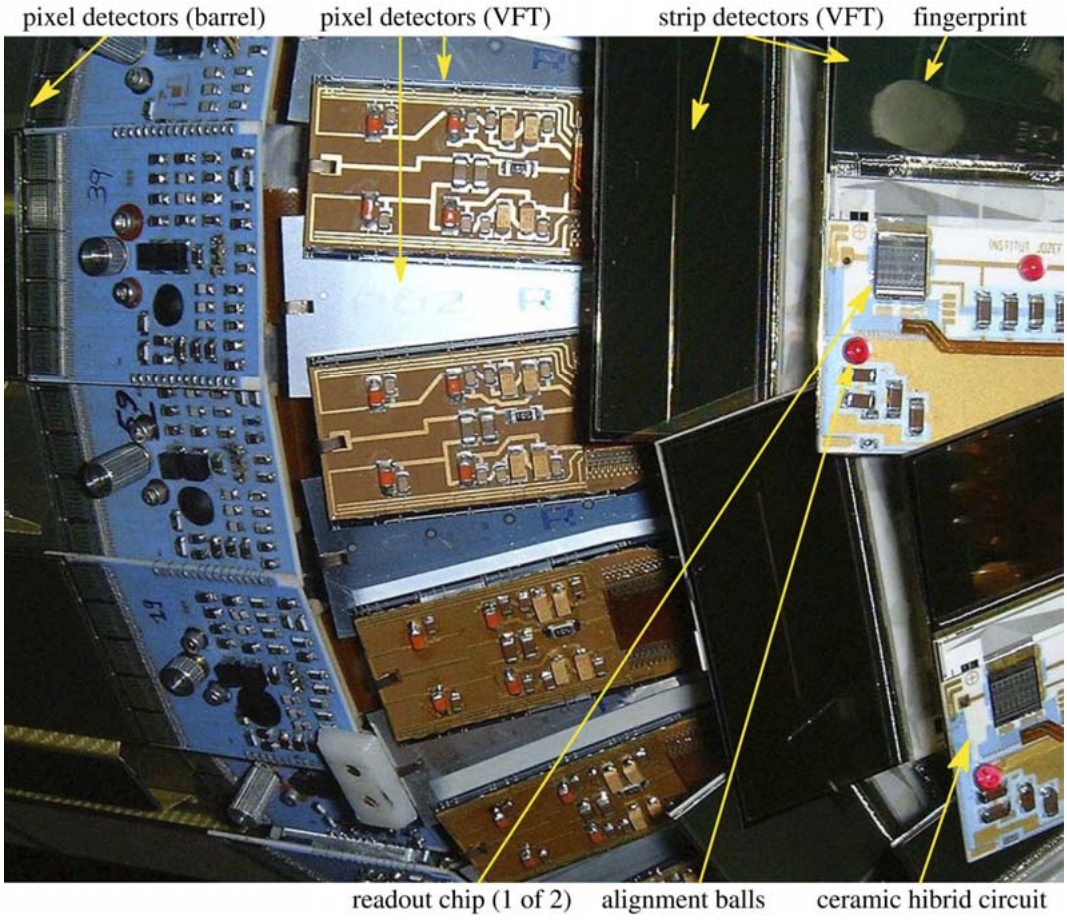


**Fig.10:** Part of the Very Forward Tracker (VFT) mounted on both ends of the central Vertex detector, as part of the upgrade of the DELPHI experiment of the old Large Electron–Positron (LEP) collider. The installation took place during 1995/96 winter shut down. Placed between the beam pipe (53 mm radius) and the inner detector (116 mm radius), the VFT covers the angles between 11° and 25° with respect to the beam direction. The VFT consists of two layers of pixel detectors, and two layers of strip detectors. The strip detectors were assembled and tested at the Experimental Particle Physics Department of the Jožef Stefan Institute [31], Ljubljana, Slovenia. After five years of successful work and greatly enhanced statistics for the weak interaction ($W^{\pm}$, and $Z^0$ bosons) the LEP was turned up to record energy levels of 209 GeV in order to search for the characteristic signature of a Higgs boson decay [32] (estimated at 115 GeV), but the results were inconclusive. In November 2000 the LEP was shut down [33] and dismantled to make way for the new LHC. The photo, taken in 2001, clearly shows a fingerprint on one of the strip detectors, left by one of the curious workers. Also easy to notice is one of the two readout chips, mounted on each ceramic hybrid circuit. The red plastic balls glued to the hybrid were used for LASER guided positioning, ensuring a mounting accuracy of less than 5 µm. In total, 48 modules were mounted, 24 on each side, each module containing 2 back-to-back strip detector pairs, resulting in 24576 readout channels. The complete upgraded Vertex Detector had ~1.2 million readout channels.

The strip detectors mounted in the VFT had a readout pitch of 200 µm and one interpolation strip between each readout pair. The detector area was 53×53 mm, thus allowing 256 readout channels per detector. Two MX6 chips, with 128 channels each performed the readout [27]. Fig.9 shows the bonding of one chip. Because of the difference in size, a ceramic fan-in had to be used in between to adapt the 45 µm double row pitch of the chip bonding pads to the 200 µm strip pitch on the detector.

In contrast with the DELPHI Vertex detector, the ATLAS Silicon Tracker [34] is much larger in both length and diameter and has four layers of detectors, as can be

seen in Fig.1, Fig.11, and Fig.15. This means that the total area covered by the detectors is much larger (~61 $m^2$). Also the pitch of both the pixel and strip detectors is finer, because of the need to provide increased spatial resolution. Consequently, the required number of readout chips is also large (~50 000 chips, 6.2 million channels).

At LEP the beam luminosity [2] was quite low, mainly owed to a relatively slow serial output data reading — after a 4μs signal integration time, all the 512 channels of each detector module (4 chips, 2 on each side) had to be shifted sequentially and digitized after each event, so collision events were repeating once every 100 μs or so. But in ATLAS, the maximum expected collision rate will reach one every 25 ns [35]. Such a high event rate is necessary because the higher the collision energy, the less probable becomes the actual head-on collision, which means that most of the time relatively uninteresting decays will occur, only a few events in a million will be of interest, passing the trigger conditions. Of those, most again will turn out to be known background. Also, the interesting events will come in large variations, and in order to acquire the required number of events for a relevant statistics in a foreseeable time, a high rate is highly desirable [36]. A high rate requires very fast readout chips, and 12 chips are required for each detector module (6 per detector, two detectors mounted back to back, see Fig.12 and Fig.13).

All these considerations result in power consumption of the order of 1.3 A per module on the analog supply at 3.5 V, and about 0.8 A on the digital supply at 4.25 V. The chips, even if each of its amplifiers would ordinarily be characterized as 'very low power', will be running quite hot. Also, as shown in Fig.11, the layout of the ATLAS SCT consists of four layers of detector modules for the 'barrel' and four rings of detector modules are mounted on each side, forming the 'forward' complex. Since this whole structure is enclosed within the Transition Radiation Tracker (TRT) and in turn in the inner detector, cooling becomes inevitable. The whole inner detector is cooled by nitrogen to −10°C.

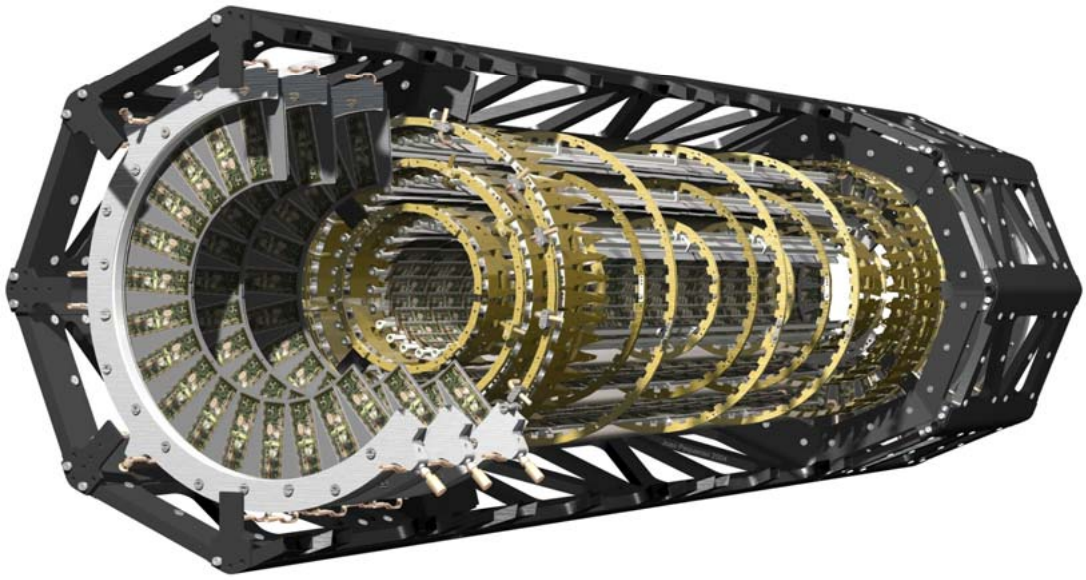

**Fig.11:** ATLAS SCT open frame. Four layers of detectors form the central 'barrel', and there are four Forward Tracker rings on each side. The barrel and the end-caps are populated with 4,088 detector modules, with a total silicon area of 61 $m^2$.

[2] Luminosity: The number of particles per square-centimeter per second in the beam.

Another problem with such a densely packed structure is the amount of material involved in the construction. It is required that the detectors are as 'transparent' as possible for the particles, reducing their energy only slightly, so that the calorimeters can measure it accurately. The frame holding the detectors can be made using low density materials, such as carbon fibre and berillium [37], but the greatest problem is the power and control wiring for the high number of modules. In addition, copper, the usual wire material, can easily become radioactive itself under high energy radiation. Needless to say, it is highly undesirable to have a material adding its own particles to the background of the very sensitive detectors. The solution is to use aluminum, which can not be activated, and reduce its thickness as much as possible.

This is where the researches at the Jožef Stefan Institute contributed another technological breakthrough, developing the tools and the technology to produce 35 µm thick aluminum tapes on a kapton foil, with 3.5 mm wide power wires and 0.5 mm control wires in lengths from 1.5 m up to 6 m, a pair for each detector module. Although similar flexible circuits were already known, with copper on kapton, used mostly in cameras and other portable electronics equipment, there were previously no facilities for producing aluminum low-mass tapes of the required thickness, length and precision. The tapes were mass produced by a Slovenian company Elgoline [38], about 4200 pairs in total. Also at Elgoline, a large number of conventional printed circuit boards were produced, supporting the required filtering and sensing components, and connectors for transition to conventional cables.

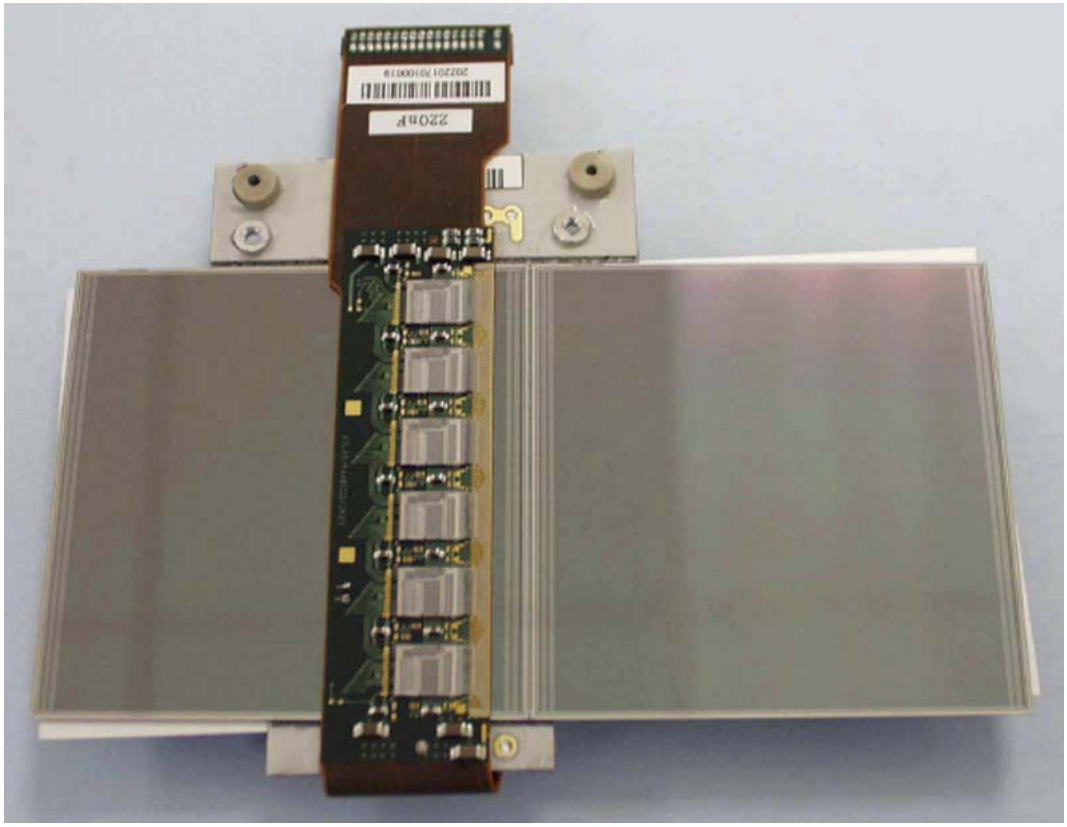

**Fig.12:** ATLAS STC Barrel detector module. The module consists of two inter-bonded pairs of identical, single-sided silicon micro-strip sensors, with 768 AC–coupled p-strips on n-type silicon, the strip pitch being 80 µm, and a total strip length of 124 mm. A total of 12 chips (6 per side), with 128 channels each, are used for readout.

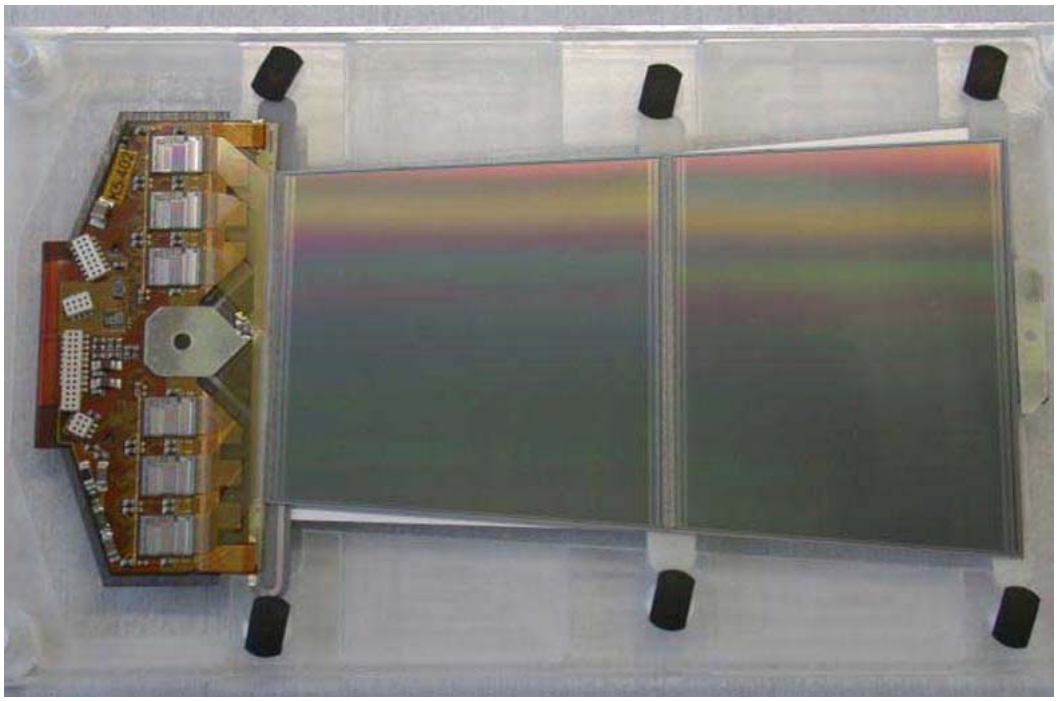

**Fig.13:** ATLAS STC Forward detector module. The detectors are of trapezoidal form, in contrast with the barrel detectors, but otherwise similar in construction. Also, the mounting diameter of the ATLAS SCT is much larger than was the DELPHI and there are four Forward rings on each side, therefore the number of detectors is much higher.

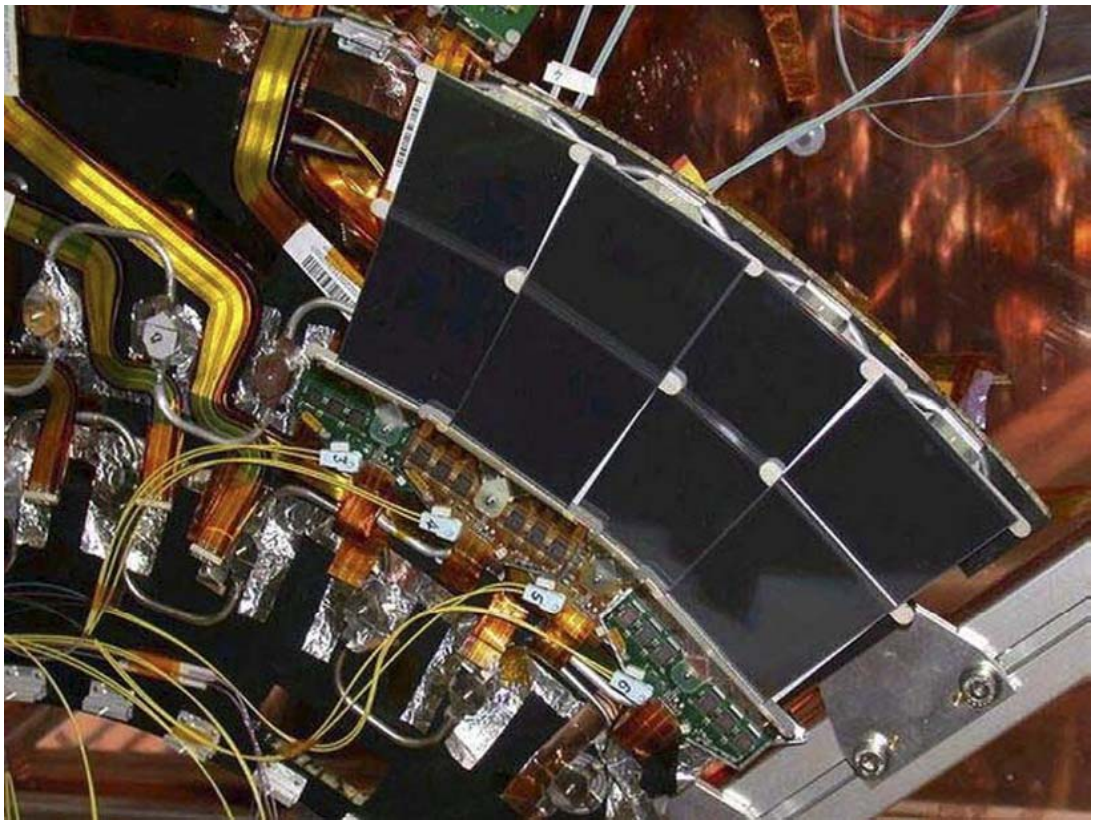

**Fig.14:** Four SCT Forward strip detectors on the test bench. The power and control come in via the wide flexible cables (aluminum on kapton foil), whilst the data transfer is done via optical links (tinny yellow cables) using a VCSEL LASER diode as the transmitter.

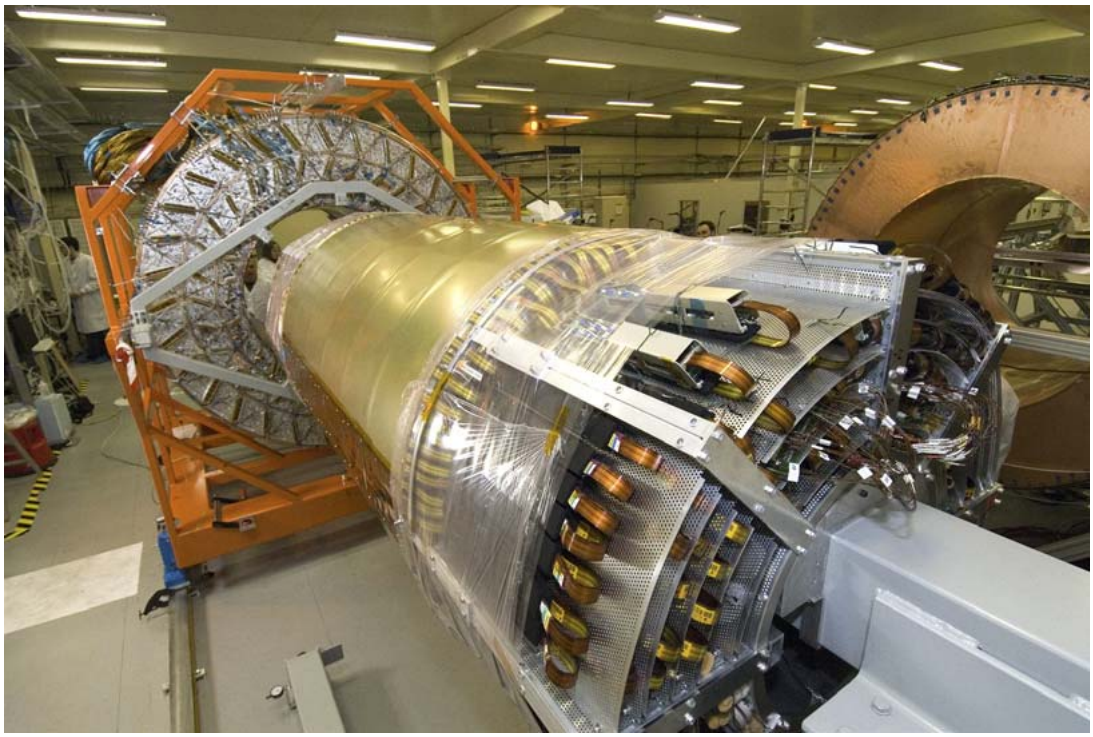

**Fig.15:** Mounting of the ATLAS Silicon Tracker (SCT) into the Transition Radiation Tracker (TRT). Note the large number of low-mass tapes providing power and control signals, one pair of tapes for each detector module.

### Input Amplifiers

Fig.16 shows the equivalent schematic diagram of a typical detector and a readout charge (transimpedance) amplifier. A quick circuit analysis is in order here, as it is important to show the difference in signal amplification on one hand, and noise sources and noise amplification on the other, in order to understand the constraints and influences of each circuit component for system optimization.

The detector consists of a diode manufactured on the silicon bulk material. This diode exhibits a structure dependent capacitance $C_d$ (2–3 pF for pixel detectors and 10–30 pF for strip detectors) and the equivalent leakage resistance $R_d$ under reverse bias by some high voltage (50–500 $V_{dc}$). The metal traces from bonding pads to the electrodes can have a few Ohms, modeled by $R_e$. The signal is capacitively coupled to the amplifier by an on-detector capacitor $C_c$ (usually a few pF). The anode is tied to ground potential by a bias resistor $R_g$ to signal ground.

The amplifier is a charge sensitive (transimpedance) configuration, with feedback impedance formed by a parallel connection of $R_{fb}$ (10–100 kΩ) and $C_{fb}$ (usually 0.2–1.0 pF, depending on the equivalent detector capacitance, a series connection of $C_c$ and $C_d$, which loads the feedback input).

The HV-bias filter capacitor $C_f$ is usually large, 10–100 nF, and for the purpose of AC gain analysis can be neglected; although, because it must withstand a relatively high voltage (from 50 V up to 500 V for modern detectors), it tends to be bulky and can have a rather high parasitic inductance, which can affect the response,

because the electrode resistance $R_e$ is usually too low to damp the $LC$ resonance. So bypassing $C_f$ by one or two lower value capacitors is necessary.

The leakage resistance $R_d$ is initially very high, but lowers with irradiation, contributing to the system noise. The noise is dominantly the '$1/f$' noise at low frequencies and white noise at high frequencies, but, owed to irradiation damage to the detector's crystal lattice and dopant concentration, the shot noise component can often become annoyingly high. Fortunately, for AC gain, $R_d$ appears effectively in parallel with $R_g$, which may be as low as a few kΩ.

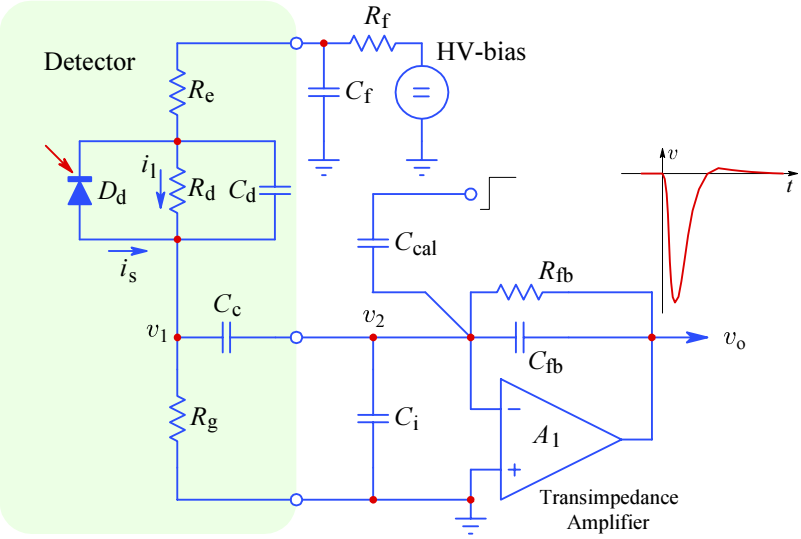


**Fig.16:** Equivalent schematic diagram of the detector with a transimpedance input amplifier. $D_d$ models the detector PN junction, $R_d$ models the detector leakage resistance, $R_e$ is the equivalent electrode and bonding resistance, and $C_d$ represents the equivalent detector capacitance (it decreases with bias voltage). All modern detectors now also contain a grounding bias resistor $R_g$, which conducts the leakage current $i_l$ to ground, and a coupling capacitance $C_c$, which couples the signal current $i_s$ to the amplifier; both $R_g$ and $C_c$ are integrated in the detector structure (older detectors needed those components to be added at the amplifier input, where the available chip area is scarce). $C_i$ is the amplifier and bonding stray capacitance, $C_{fb}$ and $R_{fb}$ are the amplifier feedback capacitance and resistance, respectively. The high voltage bias is low pass filtered by $R_f$ and $C_f$. The amplifier gain is 1 at DC, increasing at high frequencies to a value set by the feedback and grounding capacitance ratio. Modern amplifiers usually have a calibration capacitance $C_{cal}$, to which an external pulse of a few mV can be applied. It can be used for testing but its main purpose is to precisely define the system AC gain and stray capacitance.

By replacing $C_f$ and $R_e$ with a short circuit, and neglecting $D_d$ and $R_d$, we are left with $C_d$ effectively in parallel to $R_g$. Then, assuming also that the calibration capacitance $C_{cal}$ is driven from a very low impedance source (often a 1000:1 resistive voltage divider), the equivalent input impedance seen by the amplifier feedback can be calculated simply as:

$$Z_i = \frac{1}{sC_i} + \frac{1}{sC_{cal}} + \frac{1}{sC_c + \dfrac{1}{\dfrac{1}{R_g} + sC_d}} \qquad (5)$$

The amplifier's feedback impedance is:

$$Z_{\text{fb}} = \frac{1}{\frac{1}{R_{\text{fb}}} + sC_{\text{fb}}} \tag{6}$$

So the amplifier's noise gain is:

$$\frac{v_{\text{o}}}{v_n} = -\frac{Z_{\text{fb}}}{Z_{\text{i}}} \tag{7}$$

Here the noise voltage is modeled as a generator in series with the non-inverting input of the amplifier.

The detector's signal, as well as the detector's noise, originate from a different point in the circuit, the current $i_{\text{s}}$. Since the detector tends to have a large area (much larger than the amplifier's input transistors), the detector's noise usually dominates, even if the detector's noise gain is lower than that of (7).

The system transfer function can be derived from the following set of equations, starting from the sum of currents at the node $v_1$:

$$i_{\text{s}} = \frac{v_1}{\frac{1}{\frac{1}{R_{\text{g}}} + sC_{\text{d}}}} + \frac{v_1 - v_2}{\frac{1}{sC_c}} \tag{8}$$

followed with the sum of currents at the node $v_2$:

$$\frac{v_1 - v_2}{\frac{1}{sC_c}} = \frac{v_2}{\frac{1}{s(C_{\text{cal}} + C_{\text{i}})}} + \frac{v_2 - v_{\text{o}}}{\frac{1}{\frac{1}{R_{\text{fb}}} + sC_{\text{fb}}}} \tag{9}$$

and finally taking into account the amplifier's open loop gain $A_0$ and bandwidth set by the dominant pole $s_0$:

$$v_{\text{o}} = -v_2\, A_0 \frac{-s_0}{s - s_0} \tag{10}$$

By solving these equations, and eliminating $v_1$ and $v_2$ from the expression, we obtain the system transfer function in form of a fairly complex second-order transimpedance relation (in spite of having been derived from a fairly simple circuit). Usually we normalize the transimpedance to the effective input voltage $i_{\text{s}}R_{\text{g}}$, as well as sort the polynomial coefficients by falling powers of the complex frequency $s$:

$$\frac{v_{\text{o}}}{i_{\text{s}}R_{\text{g}}} = -\frac{sC_{\text{c}}R_{\text{fb}}\omega_0^2}{s^2 + s\beta + \omega_0^2 + \varepsilon(s, A)} \tag{11}$$

Here the coefficient $\beta$, which sets the response damping factor, is:

$$\beta = \frac{1}{(C_{\text{d}} + C_{\text{c}})R_{\text{g}}} + \frac{1}{C_{\text{fb}}R_{\text{fb}}\left(1 + \frac{C_{\text{c}}}{C_{\text{d}}}\right)} + \frac{1}{C_{\text{fb}}R_{\text{fb}}\left(1 + \frac{C_{\text{d}}}{C_{\text{c}}}\right)} \tag{12}$$

whilst the system cut off frequency $\omega_0$ is:

$$\omega_0 = \sqrt{\frac{1}{C_{\text{fb}} R_{\text{fb}} (C_c + C_{\text{d}}) R_{\text{g}}}} \tag{13}$$

The coupling capacitance $C_{\text{c}}$ and the feedback resistor $R_{\text{fb}}$ set the system zero.

There is also a frequency dependent error term $\varepsilon(s, A)$, owed to the limited amplifier's open loop gain $A_0$ and bandwidth $\omega_{\text{h}} = -s_0$:

$$\varepsilon = \frac{s - s_0}{-A_0 s_0} \left( s^2 \xi + s\zeta + \omega_0^2 \right) \tag{14}$$

where:

$$\xi = 1 + \frac{C_{\text{i}} + C_{\text{cal}}}{C_{\text{fb}}} + \frac{C_{\text{d}} C_{\text{c}}}{C_{\text{fb}} (C_{\text{d}} + C_{\text{c}})} \tag{15}$$

and:

$$\zeta = \frac{1}{C_{\text{fb}} \left(1 + \frac{C_{\text{c}}}{C_{\text{d}}}\right) R_{\text{fb}}} + \frac{1}{C_{\text{fb}} \left(1 + \frac{C_{\text{d}}}{C_{\text{c}}}\right) R_{\text{fb}}} + \frac{1}{C_{\text{fb}} \left(1 + \frac{C_{\text{d}}}{C_{\text{c}}}\right) R_{\text{g}}} + \frac{C_{\text{i}} + C_{\text{cal}}}{C_{\text{fb}} (C_{\text{d}} + C_{\text{c}}) R_{\text{g}}} + \frac{1}{(C_{\text{d}} + C_{\text{c}}) R_{\text{g}}} \tag{16}$$

Note that $R_{\text{fb}}$ must be chosen not to achieve a high transimpedance, but instead to provide a relatively fast system relaxation, which is important for high input pulse rates. If the system response were to exhibit a long 'tail' after each pulse, the amplitude of the following pulse would be affected by the instantaneous output value of the previous pulse, which is highly undesirable. Because of that, the system gain is set by the capacitive ratio. Of course, in order to achieve high response speed and low noise, each capacitance in the system should be made as small as possible.

Note also that the detector's noise is amplified by a factor equal to the signal gain, and since a noisy signal can affect the required trigger threshold accuracy, it is sometimes desirable to increase $C_{\text{fb}}$ beyond the response optimum, in order to reduce the high frequency noise components.

From all this it is clear that each detector–amplifier system must be highly optimized, if we are to obtain a nearly Gaussian impulse response. To allow the system designers some degree of flexibility, most chips are designed with this optimization in mind, providing a number of adjustments in form of external voltage and/or current controlled bias of various amplifier parameters, including quiescent power consumption and input amplifier speed tradeoff, several variable time constants to shape the trigger and post-trigger signals separately, and even input bias current compensation. More information on readout signal processing can be found in [39].

Fig.17 shows a typical frequency dependent gain and phase of such a system, whilst Fig.18 shows the transient (impulse) response.

The internal construction of an actual amplifier is very similar to an ordinary low-power operational amplifier, but with only the inverting input accessible externally, suitable for a transimpedance amplification. Because of the high number of amplifier channels, which need to be implemented on a single chip, it is important to choose such a circuit configuration that has high gain and linearity at low supply voltage, high speed, low output to input influence, and low transistor count.

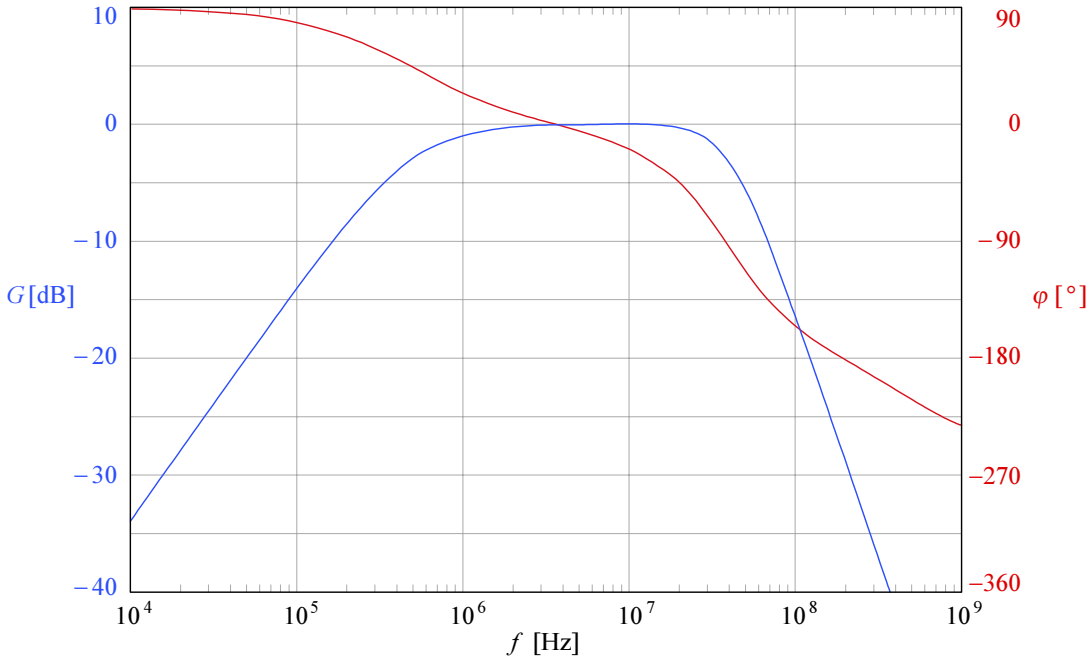


**Fig.17:** Frequency dependent gain and phase of a typical detector–amplifier system.

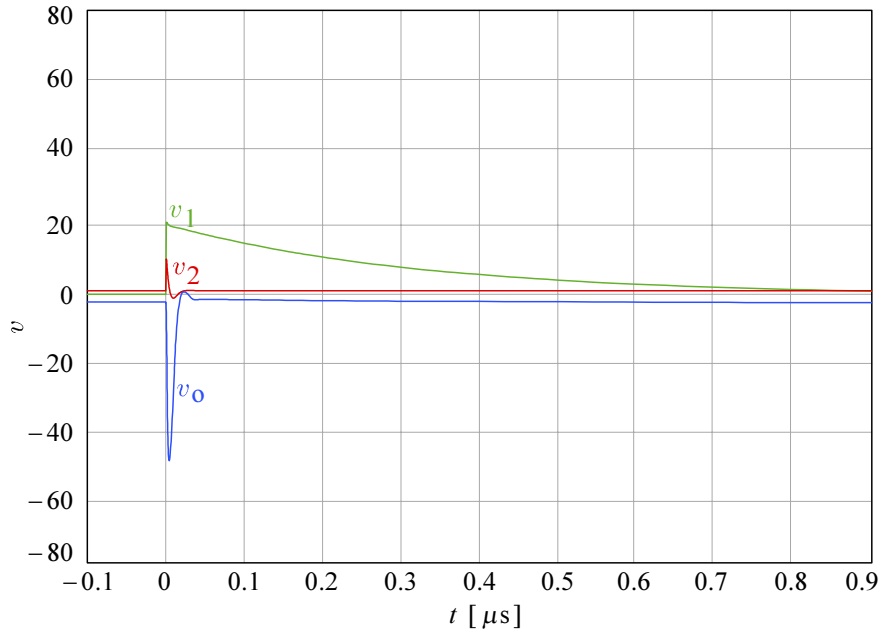


**Fig.18:** Transient (impulse) response of a typical detector–amplifier system.

Fig.19 shows the schematic diagram one of the 128 amplifiers of the MX6 readout chip, which has been used in the LEP DELPHI vertex detector (see Fig.9). MOSFET transistors $Q_1$ and $Q_3$ form a so called 'folded cascode', the drain of $Q_1$ driving the source of $Q_3$. The bias voltage $V_{\text{bias1}}$ drives the gate of $Q_2$ to set the drain current of $Q_1$ to about 200 µA, and a transconductance $g_m \approx 3\,\text{mA/V}$. The $V_{\text{bias2}}$ sets the drain current of $Q_4$ and consequently also of $Q_3$ to about 50 µA. $Q_5$ and $Q_6$ set the

gate reference voltage of $Q_3$. $Q_7$ is the current source for the output stage source-follower $Q_8$. Finally, $Q_9$ and $Q_{10}$ reset the DC level before each new measurement interval. The input network $R_1$, $D_1$, $D_2$, protects the chip from possible excessive input leakage current from the detector's high-voltage bias.

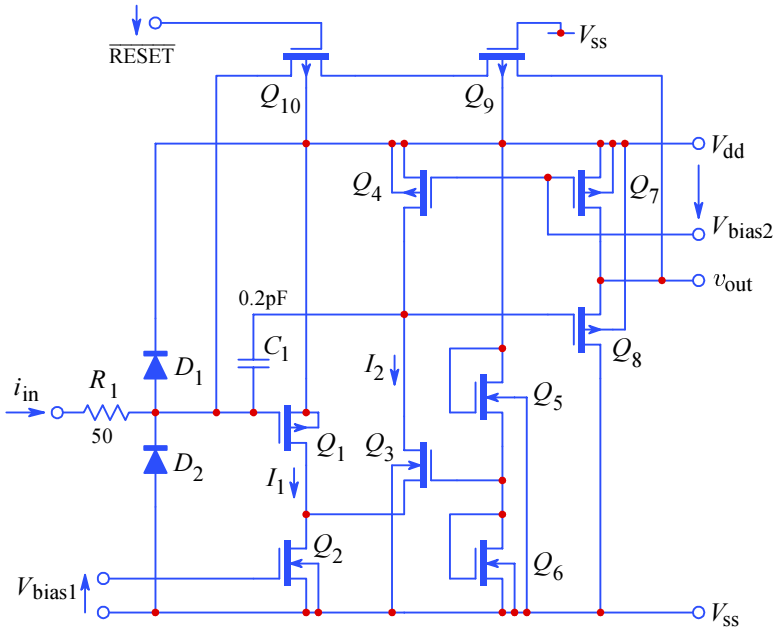


**Fig.19:** One of the MX6 chip's 128 input transimpedance amplifiers.

The feedback capacitance $C_1$ of 0.2 pF forms a capacitive divider with the parallel combination of the detector's strip capacitance and the chip's input stray capacitance of 26 pF in total, resulting in an AC gain of about 125 and a DC gain of ~800. The circuit maintains a linearity better than 1% for an input charge of $\pm 10^6$ e$^-$, whilst its input noise is equivalent to about 260 e$^-$, dominantly $1/f$. The rise time is about 150 ns (with the input detector capacitance included).

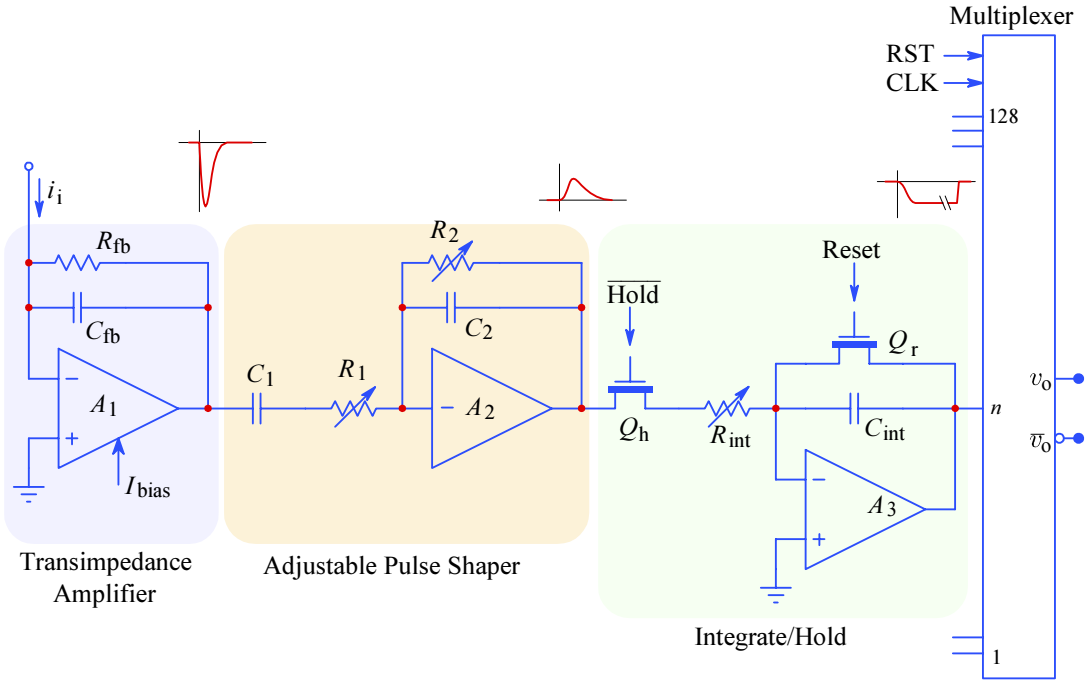


**Fig.20:** A typical readout chip front end: input signal amplification, shaping, hold and readout.

However, a multi-channel system must also perform a number of other tasks, as shown simplified in Fig.20. Most importantly, the acquired signal must be held long enough to be read, and the amplitude of the input pulse must be detected as accurately as possible. To achieve this, an $RC$–$CR$ pulse shaper is used to reduce noise, as well as adjust the pulse shape, allowing an accurate integration for a preset amount of time in the successive stage. Upon integration, the signal is disconnected and held. An analog multiplexer is then used to connect each channel one by one to the output differential amplifier. The selected channel output is digitized by an external analog-to-digital converter, and stored in computer memory for further analysis. After reading, all the channels are reset and the system is ready to acquire another input signal.

Not shown in Fig.20, a typical multi-channel system also has some on-chip control logic, which is activated by the first channel which has a signal high enough to pass the trigger qualifier. In the MX6 chip the integration time was set externally to about 2 µs after the first signal, and up to 4 µs sinchronous with the beam events. The trigger signal is usually taken from the front-end amplifiers, before the slow shapers. After the 2 µs the signal has reached a peak value, the control logic than puts the system to hold and signals a digital data-ready flag to the external control.

Many chips have also a possibility to select one channel permanently open, which makes it easier to test the various setups, to calibrate the system, check the required trigger threshold level, and to evaluate the signal to noise ratio for each channel — yes, channels can be very different in this respect.

In LEP, one important parameter was low power consumption, therefore a CMOS design was a natural choice. In contrast, the most important parameters in the LHC are response speed and radiation hardness, so bipolar technology was mandatory for the analog part. Another problem was how to deal with the extremely high data rate, and the solution adopted was local data processing. But to implement all the necessary functions within a single chip proved to be impractical at the time, so two chips were produced. The CAFE chip (‘Complementary-bipolar Analog Front-End’) [40-41] was intended for detector readout, whilst the ABC (‘Atlas Binary Chip’) [42-43] was intended mainly for data processing. Later, with the adoption of BiCMOS technology the two chips were functionally merged together on a single chip called ABCD3T, produced by ATMEL.

Fig.21 shows one of the 128 signal processors on the ABCD3T front-end. As in the MX6, here, too, a cascode input is employed, formed by $Q_1$ and $Q_2$, with $Q_8$ acting as the input protection for negative pulses. The input stage current can be set separately by adjusting the base voltage of $Q_4$. The emitter follower $Q_3$ buffers the $Q_2$ collector signal, providing low impedance drive for the following stage, as well as driving the feedback passive network $R_1||C_1$.

The following stage, formed by $Q_9$, $Q_{10}$, and $Q_{11}$, is a conventional Miller integrator. Its role is twofold: pulse shaping and generating a relatively long discharge tail. This, in connection with the comparator in the following stage, allows amplitude sampling in form of a time-over-threshold manner, so that the output is a digital pulse proportional in width to the input signal amplitude. The emitter follower $Q_{17}$ provides the low impedance to drive via $C_3$ the comparator, $Q_{15}$–$Q_{22}$, whilst the transistors $Q_{30}$–$Q_{32}$ form a digital open collector output for easy multiplexing of channels. All

the current generators can be biased externally, but an internal default is also provided.

The amplitude to pulse width conversion encodes a time stamp on both pulse edges (time-over-threshold), performing crude but efficient amplitude quantization, so that the data can be stored and processed (selected) by the next digital stage.

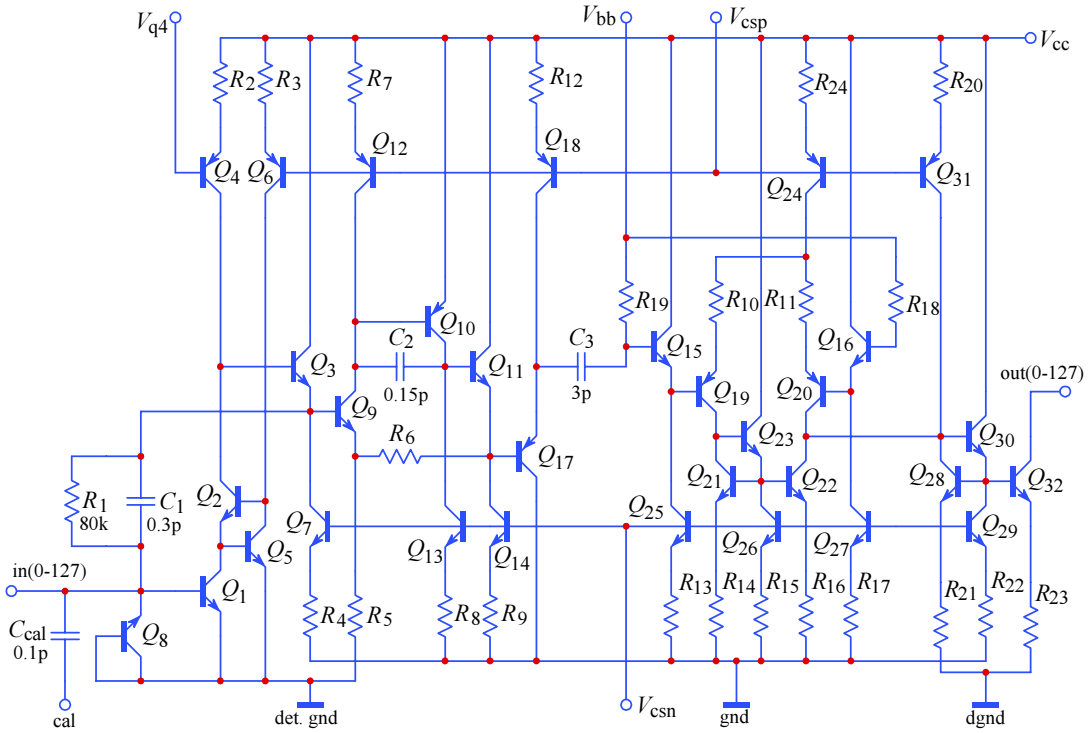


**Fig.21:** Input amplifier, integrator (shaper) and comparator (one of 128 channels) of ABCD3T chip, used in the ATLAS SCT.

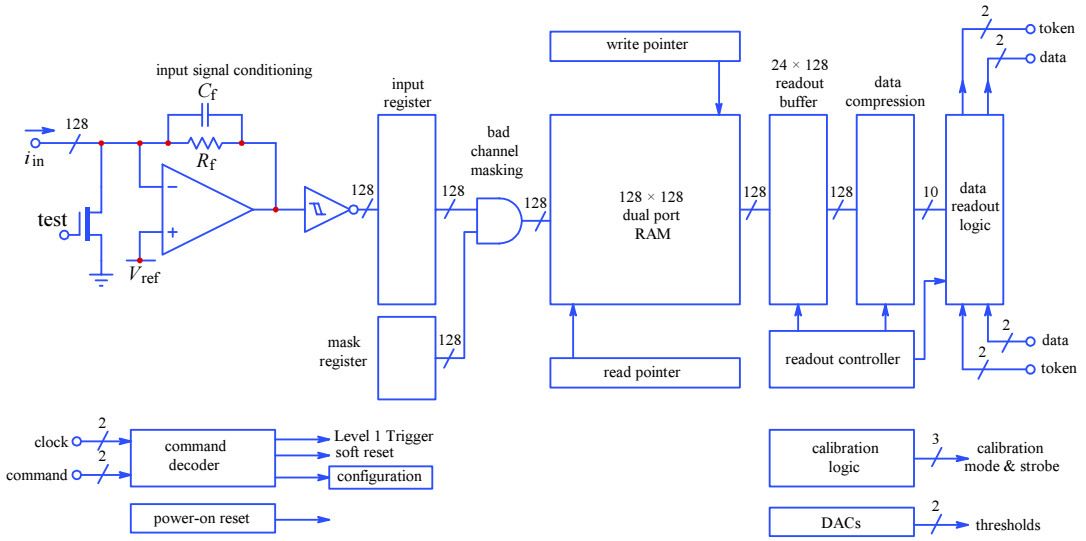


**Fig.22:** Block diagram of the ABCD3T, an evolution of both CAFE and ABC chips, used in the ATLAS SCT for detector readuot and intermediate data storage, selective triggering, and control.

The block diagram of the ABCD3T chip is shown in Fig.22. The ABCD3T was realized in BiCMOS technology. The chip provides a temporary storage in form

of a dual-port RAM, allowing independent reading and writing. The data are read from it only if the trigger condition is met, otherwise they are discarded. Enhanced digital electronics has provided a powerful trigger processor that greatly improves the trigger efficiency. In data readout systems an improved triggering also improves data throughput, whilst reducing power requirements. Furthermore, a 24 stage buffer functions as a pipeline for outgoing data. All this considerably reduces the required data throughput, which would otherwise slow down the acquisition rate.

The contemporary progress in integrated circuit technology is often measured by the continual reduction in feature size and increased functionality. However, technology by itself cannot make miracles. Under power constraints and bandwidth requirements, smaller feature sizes will not provide lower amplifier noise parameters. On the other hand, a reduction in sensor capacitance will reduce the noise charge and amplifier noise gain significantly.

Likewise, smaller CMOS feature size will not result in required electronic noise at lower power, but it will improve digital power efficiency. Smaller feature sizes reduce the size of some circuitry (not necessarily in the analog part), and this allows the implementation of additional circuitry to correct for some shortcomings. For example, small feature sizes tend to increase DC bias offsets and threshold mismatches, but facilitate the inclusion of trim DACs to correct for this. Another example is in the digitally controlled bias compensation of radiation damage, which shifts operating points [44].

Unfortunately, smaller feature sizes impose lower supply voltages, which reduce the dynamic range and place other constraints on circuit topology. As a result, the major system design challenges are constant over the years [45].

But as the readout rate gets higher, some previously lesser problems become important, like isolation of digital signals from the analog input, immunity to external pickup (power supply noise rejection), packaging of detector modules, power, and material, both in detector modules and in services. Although detectors for front-line science push the envelope, in high energy physics the systems are typically very large, complex, and expensive, so robustness, reliability, and cost are of prime consideration. Another important requirement is to be able to implement quick changes in the prototype stage, which is often inhibited by special technologies that are only accessible at mass-production scales.

So, what we call ‘advanced circuit design’ largely reduces to adapting existing techniques for incremental changes. To illustrate this point, the evolution of the most important ICs, designed specifically for application in high energy physics is shown schematically in Fig.23.

The first such IC was the MicroPlex [46]. Its power dissipation was quite high, about 10 mW/channel, so it had to operate with pulsed power, switching the supply voltages off between beam bunches. Today this is a recurring theme in designs for the International Linear Collider (ILC). Superficially, the reduction in power in the MX series of chips, the CAMEX, and SVX, has been attributed to the use of CMOS, rather than NMOS as in the MicroPlex. Although CMOS provides a significant power reduction in digital circuitry, the power dissipated in the analog input is the same. The large power dissipation in the MicroPlex was determined by the input amplifiers, which were designed with a much higher bandwidth than necessary. Because the

charge is initially integrated on the detector capacitance and then transferred into the amplifier as the charge-sensitive feedback loop becomes active [54], the bandwidth does not need to be exceptionally high. The lesson is that one must consider design requirements very carefully, optimizing system performance as a whole.

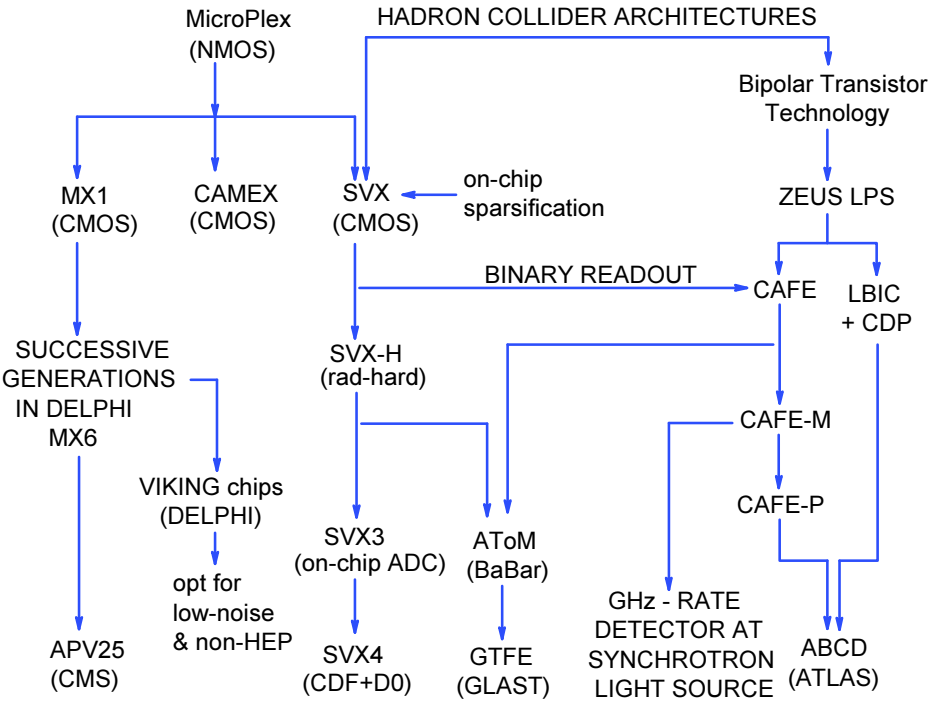


**Fig.23:** Schematic evolution of front-end ICs, from the 1980s on, as illustrated for the silicon strip detector readout. The MicroPlex chip [46] was the first to be designed purposely for high energy physics, having parallel channels of charge-sensitive amplifiers and correlated double sampling pulse shapers, read out by an analog multiplexer (like the circuit in Fig.20). Such architectural elements were common to many subsequent designs, e.g. the MX series [47] and CAMEX [48] chips used in LEP. The SVX chip for CDF [49] extended this architecture to include threshold detection and on-chip zero suppression, so only channels with hits were read out to accommodate the higher occupancy at hadron colliders. Subsequent versions of the SVX chip were implemented in rad-hard CMOS [50] and later incorporated on-chip ADCs, providing a digital only readout [51]. The Viking chips, originally designed for DELPHI [52], adopted time-invariant shaping. This, together with a lower noise than its predecessors, opened its use in non-accelerator measurements that did not provide a timing signal to synchronize the correlated double sampling. One direct descendent of the chips used at LEP is the APV chip [53], used to read out ~$10^7$ channels in the 200 $m^2$ tracker in CMS (LHC). Before 1990 bipolar transistors were too large to be implemented in dense circuitry needed for the 50 µm strip pitch detectors. The LBIC and CAFE [54-55] chips, intended at first for the Superconducting SuperCollider and then continued for the LHC, utilized more compact bipolar transistor processes that allowed denser circuitry. Both these chips used a binary readout that only registered the presence of a hit, reducing the dynamic range requirement in the front-end and lowering the output data rate, both reducing the power dissipation. Binary readout was also used by the SVX chips, although it provides analog information too, in data analysis the binary data were used primarily. Binary readout allows analog measurements for medical diagnostic purposes by utilizing threshold scans. At LEP or the Tevatron, the time between bunches was large enough to read out all the detector, so digital signal crosstalk to the analog input did not contaminate the signal. The readout design faced a new challenge as signal acquisition and data readout had to proceed simultaneously. LBIC and CAFE used a separate chip with a digital pipeline and readout. This allowed the optimum choice of technology for the analog (bipolar), and digital circuitry (CMOS).

The main challenge of detector design used currently in the LHC was the degradation of material properties under irradiation, with consequences of increased noise and lowered signal, as well as shortening the detector lifetime. The detector material properties were studied intensively by the IJS team [56-58], using its TRIGA nuclear reactor facility [59] for short time high dose accumulation. It has been discovered that by applying an increased reverse bias voltage (up to ~500 V) and lowering the temperature of the detector, an annealing process is triggered, which actually reverses part of the damage [60]. This procedure will be used in ATLAS during the winter months shut-off (since the LHC will be using nearly as much power as the nearby Geneva city, the savings in the electricity bills are notable in the budget).

For the front-end chips, the use of 'deep submicron' standard industry CMOS has extended electronics dose capability to beyond 100 Mrad. The key parameter is the use of thin gate oxides <100 nm, which accelerates the rate of electron tunneling from the gate, so that the radiation-induced holes, trapped at the silicon–oxide interface, are neutralized. In analog circuitry the operating points can be adjusted to accommodate shifts in threshold voltage, but this is not possible in digital circuits, which tends to limit overall radiation resistance.

As already mentioned, the high collision rate in the LHC (one every 25 ns at full luminosity) does not allow all data to be read out, and most of the data won't be of physical interest anyway, so a selective trigger system is used to apply filters that enhance the ratio of desired events to background events and reduce the readout rate to manageable levels. Fig.24 shows the ATLAS trigger system as an example [61]. The overall throughput is bounded at both the input, by the data transmission bandwidth from the detector, which is limited by power considerations, and the output, limited by the storage media.

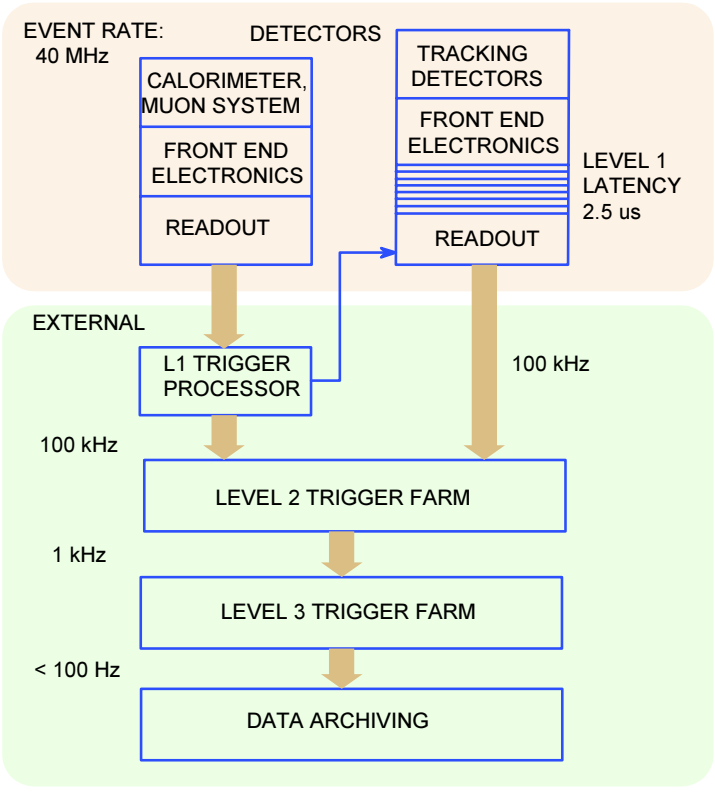


**Fig.24:** The ATLAS trigger system and the associated data rates.

**The Shiny Future**

Two future experiments characterize many of the challenges the future will pose. First, the ILC [62-65] will relax the requirements on radiation resistance and rate capability, but the vertex detectors require position resolution of order several μm to separate tracks in the cores of jets, so the pixel sizes of about 20 μm are needed near the beam. Minimizing the amount of material is critical, so power must be reduced to allow gas cooling and reduce material in power cabling. Tracking performance should be improved in the forward regions, unlike some previous collider detectors, where the forward performance has been worse than in the central region. This places severe constraints on cabling and support systems, that tend to concentrate material in the forward directions.

Secondly, the Super-LHC (sLHC) upgrade [66-70] will increase the luminosity 10× and probably reduce the bunch frequency, which will increase the number of interactions per crossing and hence the number of particle tracks to about 400. This increases requirements on pattern recognition throughout the detector and track separation close to the beam. Radiation damage in the sensors will reach levels where carrier lifetime owed to trapping will reduce signal charge, requiring a reduction in electronic noise.

Whilst silicon has proven over the years to be adaptable to a large variety of working conditions and ways of use, it has its limitations, at least for intense radiation usage. In the future we will see a shift to intrinsic rad-hard materials, such as diamond [71]. Already in ATLAS there are 12 diamond-based sensors functioning as the Beam Conditions Monitor (BCM) [7x], of which the detector studies and part of the associated electronics design were done at the Jožef Stefan Institute. Diamond, in comparison with silicon, has several advantages in terms of radiation hardness and detector stability:

- large band-gap, ~5.5eV, resulting in low leakage current;
- low relative dielectric constant, $\varepsilon_r \approx 5.7$, results in lower capacitance for the same area, thus also lower noise gain of the input transinpedance amplifier;
- high thermal conductivity, with low leakage and low noise, allows operation at room temperatures, no cooling required;
- high saturation drift velocity and high electric field breakdown enables fast signal response;
- owed to high resistance of diamond, no artificial creation of depletion region is needed to reduce the intrinsic carrier density, it is enough to make two electrodes across the material and apply a high voltage potential for high drift velocity;
- there are issues concerning polycrystalline chemical vapor deposition diamonds over mono-crystalline counterparts, the later is preferred in terms of signal efficiency, but difficult for making large areas; the problems of crystal domains, lattice distortion at boundaries, and impurities create charge trapping regions, resulting in increased leakage upon radiation, but this can be reduced by high electron irradiation ('pumping' with $\sim 10^{10}\ e^-/cm^2$ before use); this is fully reversible by exposure to UV; but pumping also has a negative side of local polarization effects, which reduce the field locally and deteriorate the signal.

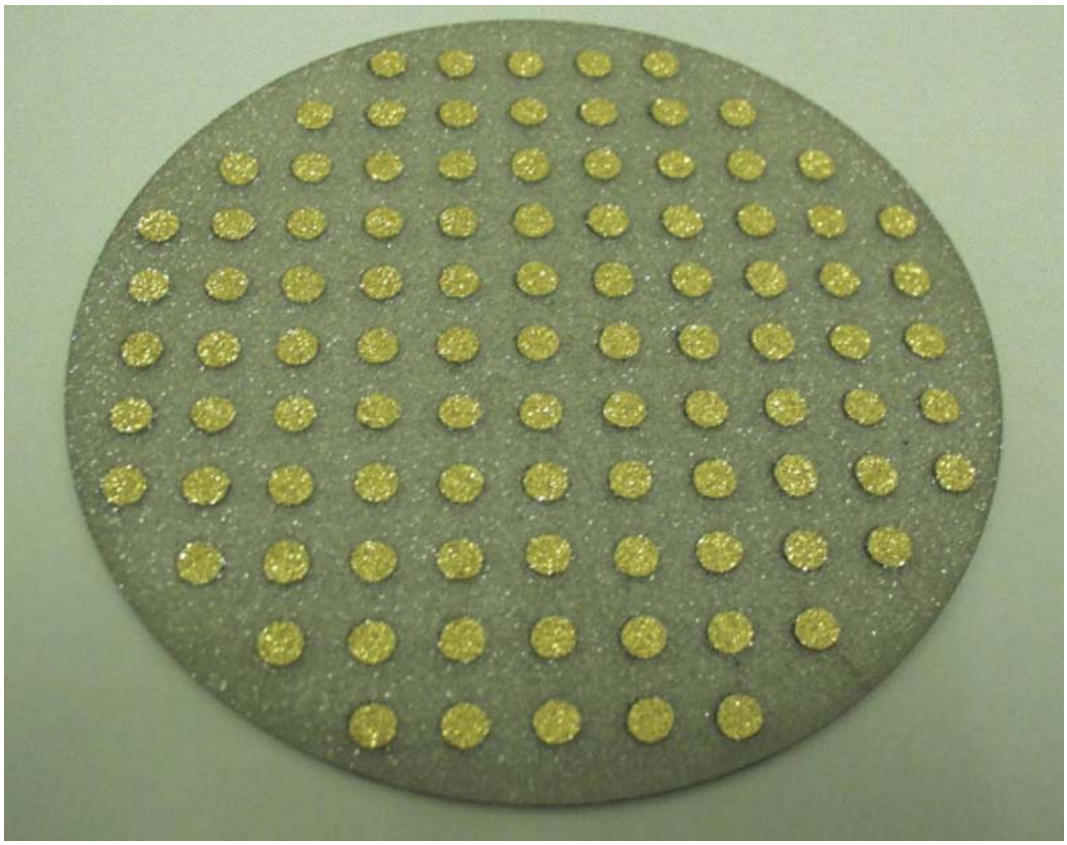

**Fig.25:** A 13cm diameter wafer of polycrystalline CVD diamond prior to dicing the BCM sensors.

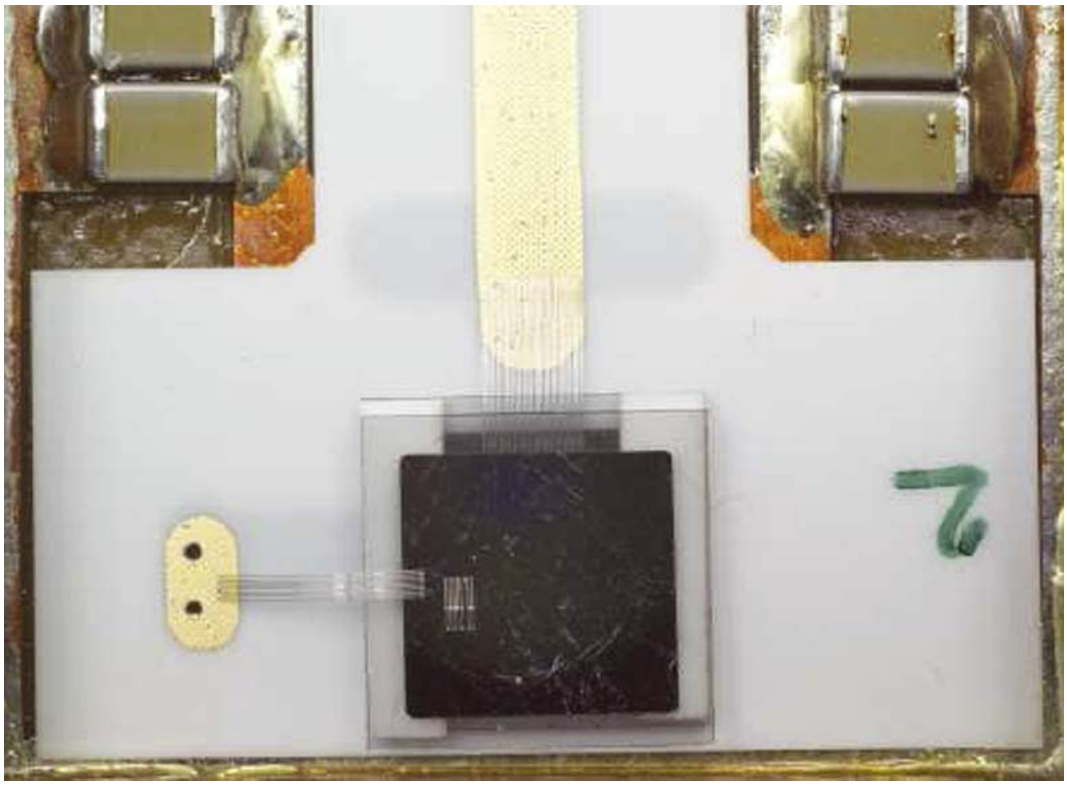

**Fig.5:** In each BCM detector two back-to-back pCVD diamond sensors are mounted on a ceramic support. The signal planes face each other in the middle of the stack, the HV bias is applied to the top and bottom. The signal planes are bonded to a transmission line (mid-top). The bonds on the left connect the HV to the top, whilst the bottom contact is made by a conductive glue to a pad.

## References

Note: There are virtually millions of documents related to high energy particle detectors; here are only a few of those of possible interest to electronics engineers; the selection criterion was, besides the content relevance, the ease of web access wherever available.


[1] CERN, [Fr.] Conseil Eurpoéen pour la Recherche Nucléaire <http://public.web.cern.ch/public/>

[2] Large Hadron Collider, LHC <https://lhc2008.web.cern.ch/LHC2008/>

[3] Micro black hole <http://en.wikipedia.org/wiki/Micro_black_hole>
More on black holes at <http://en.wikipedia.org/wiki/Black_hole>

[4] Piere Auger Observatory <http://www.auger.org/>

[5] Hawking–Beckenstein radiation <http://en.wikipedia.org/wiki/Hawking_radiation>

[6] Planck time <http://en.wikipedia.org/wiki/Planck_time>

[7] Standard Model of elementary particles <http://en.wikipedia.org/wiki/Standard_Model>
Elementary Particles <http://en.wikipedia.org/wiki/Elementary_particles>
Particle Chart <http://particleadventure.org/>

[8] $E = mc^2$ <http://en.wikipedia.org/wiki/E%3Dmc%5E2>

[9] Pair production <http://en.wikipedia.org/wiki/Pair_production>

[10] Annihilation <http://en.wikipedia.org/wiki/Electron-positron_annihilation>

[11] PET scan <http://en.wikipedia.org/wiki/PET_scan>

[12] Relativistic mass <http://en.wikipedia.org/wiki/Mass_in_special_relativity>

[13] CMB <http://en.wikipedia.org/wiki/Cosmic_microwave_background_radiation>

[14] Big Bang <http://en.wikipedia.org/wiki/Big_Bang>

[15] *S. Weinberg,* The First Three Minutes, Basic Books; 2nd Updated edition (August 17, 1993)
ISBN-10: 0465024378, ISBN-13: 978-0465024377

[16] CERN Technology transfer: Available technologies:
<http://technologytransfer.web.cern.ch/TechnologyTransfer/en/Technologies/List_of_Available_Technologies.html>
Successful transfers:
<http://technologytransfer.web.cern.ch/TechnologyTransfer/en/Successful_Transfers/Successful_Transfers.html>
Examples of technology transfer in electronics:
<http://technologytransfer.web.cern.ch/TechnologyTransfer/en/Domains/Electronics.html>

[17] The GRID <http://lcg.web.cern.ch/LCG/overview.htm>
GRID & You <http://gridcafe.web.cern.ch/gridcafe/grid&you/grid&you.html>

[18] LHC & Science <http://public.web.cern.ch/public/en/Science/Science-en.html>

[19] *K.G. McKay*, Physical Review, 84 (1951) 829

[20] *G. Bellini* et al., Nuclear Instruments and Methods, 107 (1973) 85

[21] *S.R. Amendolia*, Nuclear Instruments and Methods, 176 (1980) 449

[22] *J. Kemmer*, Nuclear Instruments and Methods, 169 (1980) 499

[23] *B.D. Hyams* et al., Nuclear Instruments and Methods, 205 (1983) 99

[24] Slilicon Vertex Detector <http://delphiwww.cern.ch/vd/>

*A. Andreazza* et al., The DELPHI Very Forward Tracker for LEP200
Nuclear Instruments and Methods in Physics Research A 367 (1995) 198-201
<http://dx.doi.org/10.1016/0168-9002(95)00541-2>

*W. Adam* et al., The status of the DELPHI very forward ministrip detector
Nuclear Instruments and Methods in Physics Research A 379 (1996) 401-403
<http://dx.doi.org/10.1016/0168-9002(96)00597-9>

[25] DELPHI Technical Proposal, CERN/LEPC/83-3, May 17th, 1983

[26] Proposal for the DELPHI Very Forward Tracker, The DELPHI Collaboration, CERN/LEPC/93-6 92-142

[27] *C. Bosio* et al., Test of a compact Si-strip detector for the forward region in DELPHI, Nuclear Instruments and Methods in Physics Research A 360 (1995) 71-74

[28] LEP & DELPHI <http://delphiwww.cern.ch/offline/physics/pubdet2.html>

[29] DELPHI <http://delphiwww.cern.ch/offline/physics/delphi-detector.html>

[30] More on the DELPHI experiment in general at: <http://delphiwww.cern.ch/offline/physics/delphi-detector.html>

[31] Experimental Particle Physics Department, Jožef Stefan Institute, Ljubljana, Slovenia <http://www.ijs.si/ijsw/Experimental_Particle_Physics_F9>

[32] *S.Stanič*, Search for charged Higgs bosons at LEP <http://merlot.ijs.si/~sstanic/delphi/index.html>

[33] LEP shut down (CERN Courier, Dec.2000): <http://cerncourier.com/cws/article/cern/28335;jsessionid=89E16BE25AD19857CE4297142B50B848>

[34] ATLAS Silicon Tracker (SCT), Endcap Module Page <http://atlas.web.cern.ch/Atlas/GROUPS/INNER_DETECTOR/SCT/ecmod/>

[35] SCT-BM, Final Design Review <http://atlas.web.cern.ch/Atlas/GROUPS/INNER_DETECTOR/SCT/module/SCTSGmod/FDR/SCT-BM-FDR-1-May13.pdf>

[36] e-Tours: <http://atlas.ch/etours.html> e-Tours: Detectors <http://atlas.ch/etours_exper/index.html> e-Tours: Physics <http://atlas.ch/etours_physics/index.html>

[37] Spine <http://wwwatlas.mppmu.mpg.de/atlas_sct/spine_fdr.pdf>

[38] Elgoline PCB production <http://www.elgoline.si/>

[39] *H.Spieler*, Analog and Digital Electronics for Detectors, Proceedings of the 2003 ICFA School on Instrumentation, Itacuruca, Brazil <http://www-physics.lbl.gov/~spieler/ICFA_Rio_2003/text/Analog_and_Digital_Electronics_for_Detectors.pdf>

[40] CAFE: User's Guide, Release 0, 26 May 1995 <http://scipp.ucsc.edu/groups/atlas/elect-doc/cafe-manual.pdf> <http://scipp.ucsc.edu/groups/atlas/elect-doc/CAFE-P_Spec.pdf>

[41] ATLAS-SCT Bipolar Amplifier-Discriminator IC Specification V4.01, CAFE-P, 13-Jan-1999 <http://scipp.ucsc.edu/groups/atlas/elect-doc/abcd3t_spec.pdf>

[42] ATLAS Binary Readout IC (ABC) Specification V5.01 21-Jul-1999 <http://scipp.ucsc.edu/groups/atlas/elect-doc/ABC_Spec.pdf>

[43] *F. Campabadal* et al., Design and performance of the ABCD3TA ASIC for readout of silicon strip detectors in the ATLAS semiconductor tracker, 2005, <http://escholarship.lib.okayama-u.ac.jp/cgi/viewcontent.cgi?article=1000&context=nuclear_physics>

[44] *F. Anghinolfi*, Radiation Hard Electronics, <http://rd49.web.cern.ch/RD49/MaterialRadCourse/FAnghinolfi.pdf>

[45] *R. Yarema*, Proceedings of the 12th Workshop on Electronics For LHC and Future Experiments LECC 2006, <http://doc.cern.ch/yellowrep/2007/2007-001/p71.pdf>

[46] *J.T. Walker* et al., Nucl. Instr. and Meth. A 226 (1984) 200

[47] *P. Seller*, *P. Allport*, *M. Tyndel*, IEEE Trans. Nucl. Sci. NS-35 (1988) 176 –180

[48] *W. Buttler* et al. Nucl. Instr. and Meth. A273 (1988) 778-783

[49] *S.A. Kleinfelder* et al., IEEE Trans. Nucl. Sci. NS-35 (1988) 171

[50] *C. Haber*, Nucl. Instr. and Meth. A471 (2001) 12-17

[51] *M. Garcia-Sciveres* et al., Nucl. Instr. and Meth. A435 (1999) 58-64

[52] *O. Toker* et al., Nucl. Instr. and Meth. A340 (1994) 572-579

[53] *M.J. French* et al., Nucl. Instr. and Meth. A466 (2001)359-365

[54] *E. Spencer* et al., A fast shaping low power amplifier-comparator integrated circuit for silicon strip detectors, Proc. IEEE Nuclear Science Symposium, 1994.

[55] *I. Kipnis*, *H. Spieler*, *T. Collins*, An analog front-end bipolar-transistor integrated circuit for the SDC silicon tracker, IEEE Transa. on Nuclear Science, vol. 41, no. 4, pp. 1095-1103, Aug. 1994.

[56] Electronics Irradiation Results <http://www-f9.ijs.si/~mandic/ElectronicsIrrad.html>

[57] Irradiation Studies Papers <http://krambi.ijs.si/gregor/papers.html>

[58] Chip Irradiation Results <http://www-f9.ijs.si/~mandic/ChipIrrad/spo233/spo233.html>

[59] IJS Reactor Center <http://www.ijs.si/ijsw/Reactor_Physics_F8>

[60] *V. Cindro*, *G. Kramberger*, *M. Mikuz*, *D. Zontar*, Bias-Dependent Annealing of Radiation Damage in Neutron-Irradiated Silicon $p^+$–n–$n^+$ Diodes, <http://krambi.ijs.si/gregor/papers/bideplet1.pdf>

[61] ATLAS SCT L1 Trigger Latency Budget <http://scipp.ucsc.edu/groups/atlas/elect-doc/SCT_L1_Latency_Spec.pdf>

[62] International Linear Collider <http://www.linearcollider.org/cms/>

[63] What is ILC? <http://www.linearcollider.org/cms/?pid=1000000>

[64] ILC wiki <http://en.wikipedia.org/wiki/International_Linear_Collider>

[65] ILC at Fermilab <http://ilc.fnal.gov/>

[66] SuperLHC detectors <http://www.cai.uu.se/workshop/15-tord-SuperLHC.pdf>

[67] Rad-Hard Detectors for sLHC <http://docs.lib.purdue.edu/physics_articles/123/>

[68] Rad-Hard Detectors for sLHC <http://cat.inist.fr/?aModele=afficheN&cpsidt=16727557>

[69] Rad-Hard Detectors for sLHC <http://eprints.lancs.ac.uk/10038/>

[70] *M. Bruzzi* et al., Radiation-hard semiconductor detectors for SuperLHC Nuclear Instruments and Methods in Physics Research A 541 (2005) 189–201 <http://sirad.pd.infn.it/people/candelori/Articoli-PDF/PC18_NIMA_2005_04_Candelori_RD50.pdf>

[71] Diamond Detectors: RD-42 Conference Presentations <http://indico.cern.ch/conferenceDisplay.py?confId=41466>

[xx] RAD-Monitor <http://www-f9.ijs.si/~mandic/RADMON/atlas_radiation_monitor.htm>

---

Additional interesting pages:

[xx] ATLAS home page <http://atlas.ch/>

[xx] ATLAS events simulations <http://atlas.ch/photos/events.html>

[xx] ATLAS photo galery <http://atlas.ch/photos/index.html>

[xx] ATLAS Electronics Documents <http://scipp.ucsc.edu/groups/atlas/sct-docs.html>

[xx] ATLAS Electronics at LBNL <http://www-atlas.lbl.gov/pixel/doc/Electronics.html>

[xx] Wire Bondong Guidelines <http://extra.ivf.se/ngl/A-WireBonding/ChapterA2.htm>
[xx] *J.P. Bizzell*, Wire Bondong, Barrel <http://hepwww.rl.ac.uk/atlas-sct/jpb/atlasbarrel.pdf>
[xx] *J.P. Bizzell*, Wire Bondong, Forward <http://hepwww.rl.ac.uk/atlas-sct/jpb/atlasforward.pdf>